Ecological Processes
a SpringerOpen Journal

RESEARCH Open Access

Combining in-situ water quality and remotely sensed data across spatial and temporal scales to measure variability in wet season chlorophyll-a: Great Barrier Reef lagoon (Queensland, Australia)

Michelle J Devlin[1*], Eduardo Teixeira da Silva[1], Caroline Petus[1], Amelia Wenger[1,2,3], Daniel Zeh[1], Dieter Tracey[1], Jorge G Álvarez-Romero[2] and Jon Brodie[1]

Abstract

Introduction: Combining in-situ data from single-point time series with remotely sensed spatial data allowed a greater elucidation of changes in chlorophyll-a concentrations through wet season conditions in the Great Barrier Reef coastal waters.

Methods: Single-point time-series data were collected from 2006 to 2012 during high river flow conditions to assess changes in phytoplankton biomass (measured as chlorophyll-a). Additionally, three flood plume water types, derived from classified true-colour Aqua moderate resolution imaging spectroradiometer (MODIS) images, were used to group single-point time-series data for the phytoplankton biomass assessment.

Results: Survey data illustrate the heterogeneity of chlorophyll-a distribution over seasonal and inter-annual cycles and the difficulty in describing community responses through the wet season. The spatial data demonstrate distinct regional differences throughout the Great Barrier Reef. The high chlorophyll-a concentrations measured in flood plume waters immediately adjacent to the inshore, highly turbid 'inner' flood plume are a product of sufficient light, given most of the suspended solids have settled from the plume, and the availability of sufficient nutrients, which drive higher phytoplankton production and characterise the formation of secondary stage flood plumes. The formation and extent of these secondary flood plumes were mapped using MODIS true-colour satellite imagery. The distance and the location of the secondary plume water are reliant on flow, coastal hydrodynamics, and biological activity.

Conclusions: The combination of in-situ data and remotely sensed data provides information on the complexity of these coastal processes during the wet season and offers managers a more comprehensive understanding of the extent of nutrient enrichment in the Great Barrier Reef coastal area and the potential influence of flood plumes on coastal marine ecosystems.

Keywords: Chlorophyll-a; Great barrier reef; Phytoplankton; Monitoring; Remote sensing; MODIS

Introduction

The primary biological response to nutrient enrichment in aquatic environments, given suitable conditions such as light availability and water temperatures, is the growth of phytoplankton and higher plants. Known consequences of nutrient enrichment on the phytoplankton community can be measured by elevated phytoplankton biomass (Boynton et al. 1996; Bricker et al. 2003; Brodie et al. 2007) and alterations of the natural phytoplankton community composition, which may in turn change ecosystem food web and nutrient cycling dynamics (Cloern 2001; Brodie et al. 2005; Devlin et al. 2009).

The understanding of nutrient enrichment and potential eutrophication in the Great Barrier Reef (GBR) has progressed in recent years with key publications identifying responses to nutrient loading for corals (Fabricius

* Correspondence: michelle.devlin@jcu.edu.au
[1]Catchment to Reef Research Group, TropWater, James Cook University, Townsville, QLD, 4811, Australia
Full list of author information is available at the end of the article

2005, 2011; Brodie et al. 2011, 2012) and seagrasses (Schaffelke et al. 2005; Collier et al. 2012; McKenzie et al. 2010), as well as phytoplankton communities (Furnas et al. 2005; Sorokin and Sorokin 2010; see references in Devlin et al. 2013). The nutrients introduced or released during high flow river discharge into the GBR are rapidly taken up by pelagic and benthic algae, and microbial communities (Alongi and McKinnon 2005), sometimes nourishing short-lived phytoplankton blooms and high levels of organic production (Furnas 1989; Furnas et al. 2005, 2011). This organic matter is cycled through the marine food web and transformed, for example, into marine snow particles that may be deposited onto benthic communities, such as coral reefs, thus influencing their structure, productivity, and health (Anthony and Fabricius 2000; Fabricius and Wolanski 2000). Further, Brodie et al. (2005) and Fabricius et al. (2010) identify enhanced nutrient supply in river runoff as a critical requirement for enhanced *Acanthaster planci* (commonly known as the crown-of-thorns starfish or COTS) larval survival in the GBR, a finding that supports Lucas' (1982) hypothesis that COTS suffer high levels of larval starvation in the absence of phytoplankton blooms. COTS are of great importance in the GBR as a predator on coral and are recognised as one of the leading causes of mid-shelf coral mortality in the GBR (De'ath et al. 2012).

Measurement of chlorophyll-a (hereafter chl-a) concentrations derived from phytoplankton biomass can be indicative of enhanced nutrient inputs (Spencer 1985; Furnas et al. 2005; Brodie et al. 2007) and thus provides a simple, reliable indicator of water column nutrient status in the absence of high frequency water column nutrient concentration measurements (Harding and Perry 1997; Yunev et al. 2002). Chl-a concentrations in the GBR waters have been successfully utilised as a proxy measurement of phytoplankton biomass and nutrient concentrations for a number of monitoring programs in the past (Brodie and Furnas 1994; Brodie et al. 1997, 2007; Furnas and Brodie 1996; Steven et al. 1998).

The frequency of in-situ sampling methods is associated with cost, time, weather, and logistic constraints and only a limited number of sampling points can be monitored during any one flood event. This restriction might limit the assessment of the range and variability of coastal processes and water constituents (Novoa et al. 2012). Conversely, satellite sensors provide an effective means for frequent and synoptic water quality observations over large areas. Remotely sensed data (e.g., derived ocean colour products) have increasingly become a tool by which scientists and managers can supplement long-term monitoring datasets of in-situ water quality measurements (Brando et al. 2010; Kennedy et al. 2012; Schroeder et al. 2012; Devlin et al. 2012b). Remotely sensed data have thus provided an essential source of information related to the movement and composition of flood plumes in GBR waters, extending the utility of the in-situ sampled data at both regional and temporal scales.

Assessing chl-a concentrations with remotely sensed data in optically complex coastal waters, such as the GBR coastal waters, where suspended sediment and coloured dissolved organic matter (hereafter CDOM) co-occur with phytoplankton, is notoriously difficult (e.g., Gitelson et al. 2009; Odermatt et al. 2012). The standard and global bio-optical algorithms used in oceanic waters (Case 1 waters; Morel and Prieur 1977; Gordon and Morel 1983; Morel 1988) are inaccurate when applied to optically complex coastal waters (Case 2 waters; Morel and Prieur 1977; Gordon and Morel 1983; Morel 1988), although regional parameterisation of these algorithms can help increase their accuracies (Naik et al. 2013; Brando et al. 2012). Some recent studies have investigated the use of remote-sensing products in the mapping of water quality parameters, particularly the use of chlorophyll and CDOM products, both for global and regional assessments (Devlin et al. 2012b; Brando et al. 2010, 2012; Schroeder et al. 2012). However, the retrieval of chlorophyll data based on the application of bio-optical algorithms (e.g., Level 2, chl-a product) is still problematic in Case 2, turbid nearshore waters (Wang and Shi 2007; Gitelson et al. 2009; Odermatt et al. 2012).

Our study utilises the variation in ocean colour to map the gradient in water quality concentrations across flood plumes to avoid these inherent problems of retrieving chl-a measurements in Case 2 waters. The same approach has been applied to map flood plumes using moderate resolution imaging spectroradiometer (MODIS) imagery, allowing assessment of their extent and influence on GBR ecosystems (Bainbridge et al. 2012; Brodie et al. 2010; Devlin et al. 2012a, b; Schroeder et al. 2012; Álvarez-Romero et al. 2013).

Our study extends earlier work on spatial and temporal patterns of chl-a distribution in the GRB (Steven et al. 1998; Brodie et al. 2007) with an analysis of a long-term dataset of chl-a concentrations collected in high flow conditions between December to April (wet season) from 2006 to 2013. This paper presents in-situ chl-a measurements sampled over variable conditions associated with the North Queensland wet season, coupled with spatial mapping outputs derived from MODIS true-colour images. The method applied in this work allowed us to assess the extent and characteristics of the dominant water of the flood plumes, without depending on the retrieval of Level 2 MODIS data in Case 2 waters. The information on the spatial extent of different flood plume water types, integrated with high frequency wet season sampling, provides a valuable tool from the environmental management perspective to assess the extent of the spatial and temporal distribution of chl-a

concentrations and, hence, phytoplankton biomass in the Great Barrier Reef.

Methods

Study area

The Great Barrier Reef extends approximately 2,000 km parallel to the Queensland east coast between 9˚S and 24˚S and covers approximately 350,000 km^2. An inner shelf area with water depths of up to 20 m is immediately adjacent to the coast. This area contains coastal and island fringing reefs and intertidal and shallow water seagrass beds. The inshore area is significantly affected by adjacent coastal influences, and its sediments are composed of predominantly terrestrial-sourced material (Brodie et al. 2012).

In-situ data collection

Data have been collected as part of the water quality program under the Reef Rescue Marine Monitoring Program (hereafter RRMMP), which aims to investigate the influence of terrestrial runoff on inshore GBR water quality (Johnson et al. 2011; Devlin et al. 2011). Water samples for this work were collected along four regions of the northeastern Australian coast within the Great Barrier Reef: the Tully (18˚S) and Herbert (18.5˚S) regions, within the wet tropics area and the Burdekin (19.5˚S) and Fitzroy (23.5˚S) regions, within the dry tropics (Figure 1). Discrete regional cross-shelf transects were monitored within each region during the wet season (ca. December to April) from 2006 to 2013. Sampling was initiated at the onset of the wet season, targeting the period after first flush, the rise, peak and flux of high river flow conditions. In addition, sampling continued through the wet season through variable flow conditions and water characteristics. The sampling dates were determined by logistics such as prevailing weather conditions and the location of the flooding rivers. The intensity of sampling varied between regions in relation to the logistics of sampling and the frequency of high flow periods. The design of the flood monitoring program under the current Marine Monitoring Program is detailed in Devlin et al. (2011).

Water sampling focused on the top surface layer of the flood plumes. Sampling within flood plumes included the collection of water samples for the analysis of total suspended sediment (TSS), chl-a, salinity, and the diffuse attenuation coefficient of photosynthetically active radiation (K_dPAR).

Surface water for chl-a and TSS was collected using a clean polyethyelene bucket, with 1 L collected for TSS and 1 L collected in a dark bottle for chl-a. Both bottles were stored in cold and dark conditions for posterior filtration. Within 12 h of sampling, water for chl-a determination was filtered through a 47 mm Whatman GF/F glass-fibre filter (0.7-μm nominal pore size) with the addition of approximately 0.2 ml of magnesium carbonate. Filters were wrapped in aluminium foil and frozen. Pigment determinations from acetone extracts of filters were done using the spectrophotometry method described in 'Standard Methods for the Examination of Water and Wastewater, 10200 H. Chlorophyll'. Within 24 h, water for TSS analysis was passed through a pre-weighed 0.45-μm Millipore filter. After collection of suspended material, filters were rinsed with MilliQ water to remove salt. Filters were dried to a constant weight, and the concentration of suspended sediment was determined by gravimetric method as presented in 'Standard Methods for the Examination of Water and Wastewater, 2540 D. Total Suspended Solids Dried at 103–105°C'.

In addition to the water samples, depth profiles using a conductivity-temperature-depth (CTD) probe from Sea-Bird Electronics (SBE-19Plus) equipped with sensors for temperature, salinity, depth, and light were also carried out. The CTD probe was kept for 3 min at the water surface for sensor stabilisation before starting the downcast. Salinity and temperature reported for the first 0.5 m of depth were calculated as the average of readings between 0.3 and 0.7 m below the water surface; outliers were identified, prior to the timing of the stabilisation period, through sharp changes in salinity that occurred if the probe accidently touched to the sea floor. K_dPAR readings were calculated using the Lambert-Beer Equation (Dennison et al. 1993). Further details on QC/QA procedures for all laboratory analyses are documented in GBRMPA (2012).

Influence of flow and salinity on the chl-a and WQ concentrations

Daily flow records from 35 stations distributed throughout the GBR were obtained from the Department of Environment and Resource Management (Queensland, http://watermonitoring.derm.qld.gov.au/host.htm). For a hydrologic characterisation of the sampling period, the total annual flow was compared against the long-term annual median flow calculated for the period 1970–2001. Annual flow volume was calculated considering a hydrological year from 1 October to 30 September.

The influences of flow and salinity were investigated as correlative factors driving chl-a concentration. On a regional scale, the in-situ chl-a data were compared among the four regions studied (i.e., Tully, Hebert, Burdekin, and Fitzroy regions) by grouping the data in terms of salinity classes and runoff regimes. To do that, the discharges on the sampling dates from the closest river to the sampling site were grouped in terms of runoff percentile. Percentiles of 5, 25, 50, 75, and 95% were calculated from the long-term data record (i.e., January 1997 to April 2013) taking into account 5-day average runoff from the sample date of the river system visited (i.e., the Tully, Hebert, Burdekin, or Fitzroy rivers). The 5-day average was arbitrarily selected as a way to represent a potential delay between the

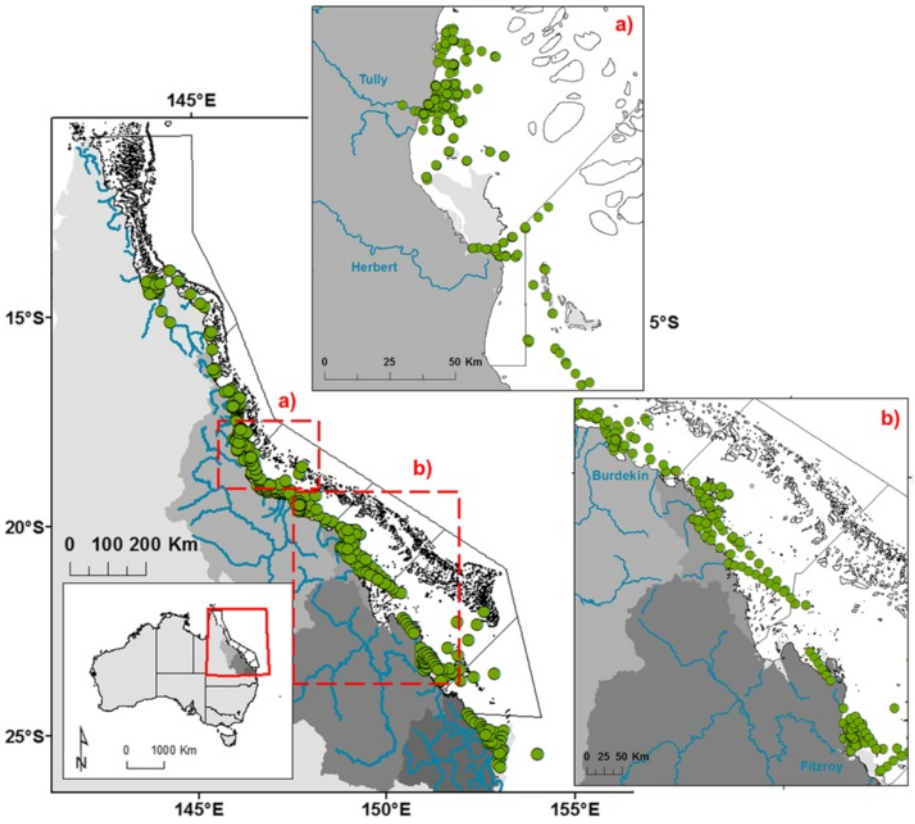

Figure 1 Location of sampling data for the period 2006–2013 for all regions. (a) The Tully (18°S) and Herbert (18.5°S) regions, within the wet tropics area, and **(b)** the Burdekin (19.5°S) and Fitzroy (23.5°S) regions within the dry tropics for the Tully marine area. For management purposes the catchment of the GBR was subdivided into five natural resource management (NRM) regions (black lines). These NRM regions extend seaward and are limited by the GBR Marine Park boundary.

river gauge measurements (average distance ~60 km from the river mouth) and the time it would take water to reach the closest sampling site (within 5–10 km from river mouth). In-situ salinity data were grouped within intervals of 10 (i.e., < 10, 10–20, 20–30, and > 30). In-situ chl-a data for each region were then characterised by runoff and salinity groups using box plots. In addition, chl-a data were plotted against guidelines for testing the reliability of chl-a measurements under the wet season conditions.

Mapping the water types in flood plumes

Flood plumes were mapped in this work using the method presented in Álvarez-Romero et al. (2013). In this method, daily MODIS Level-0 data acquired from the NASA Ocean Colour website (http://oceancolour.gsfc.nasa.gov) are converted into quasi-true-colour images with a spatial resolution of 500 × 500 m using the SeaWiFS Data Analysis System (SeaDAS; Baith et al. 2001). The true-colour image is then spectrally enhanced (from red-green-blue to hue-saturation-intensity colour system) and classified to six colour categories through a supervised classification using spectral signatures from plume water in the GBR. The six colour classes are further reclassified into three flood plume water types (primary, secondary, tertiary) corresponding to the three water types defined by Devlin and Schaffelke (2009) and Devlin et al. (2012a). Figure 2 presents a diagram of the method described within Álvarez-Romero et al. (2013) with some intermediary-step images, and Table 1 presents a description of these plume water types and how they relate to the six colour classes derived from the Álvarez-Romero et al. (2013) method. The sediment-dominated waters or primary water type were defined as corresponding to colour classes 1 to 4 of Álvarez-Romero et al. (2013). The chl-a-dominated waters or secondary water type were defined as corresponding to the bluish-green waters (i.e., colour class 5 from Álvarez-Romero et al. 2013) and the tertiary water type was defined as corresponding to the colour class 6 of Álvarez-Romero et al. (2013) (see Table 1 and Figure 2). This supervised classification was used to classify 5 years of daily MODIS images [from December 2007 to April 2012, focused on the summer wet season (i.e., December to April inclusive].

Weekly composite images were created to minimise the image area contaminated by dense cloud cover and intense sun glint (Álvarez-Romero et al. 2013). Weekly

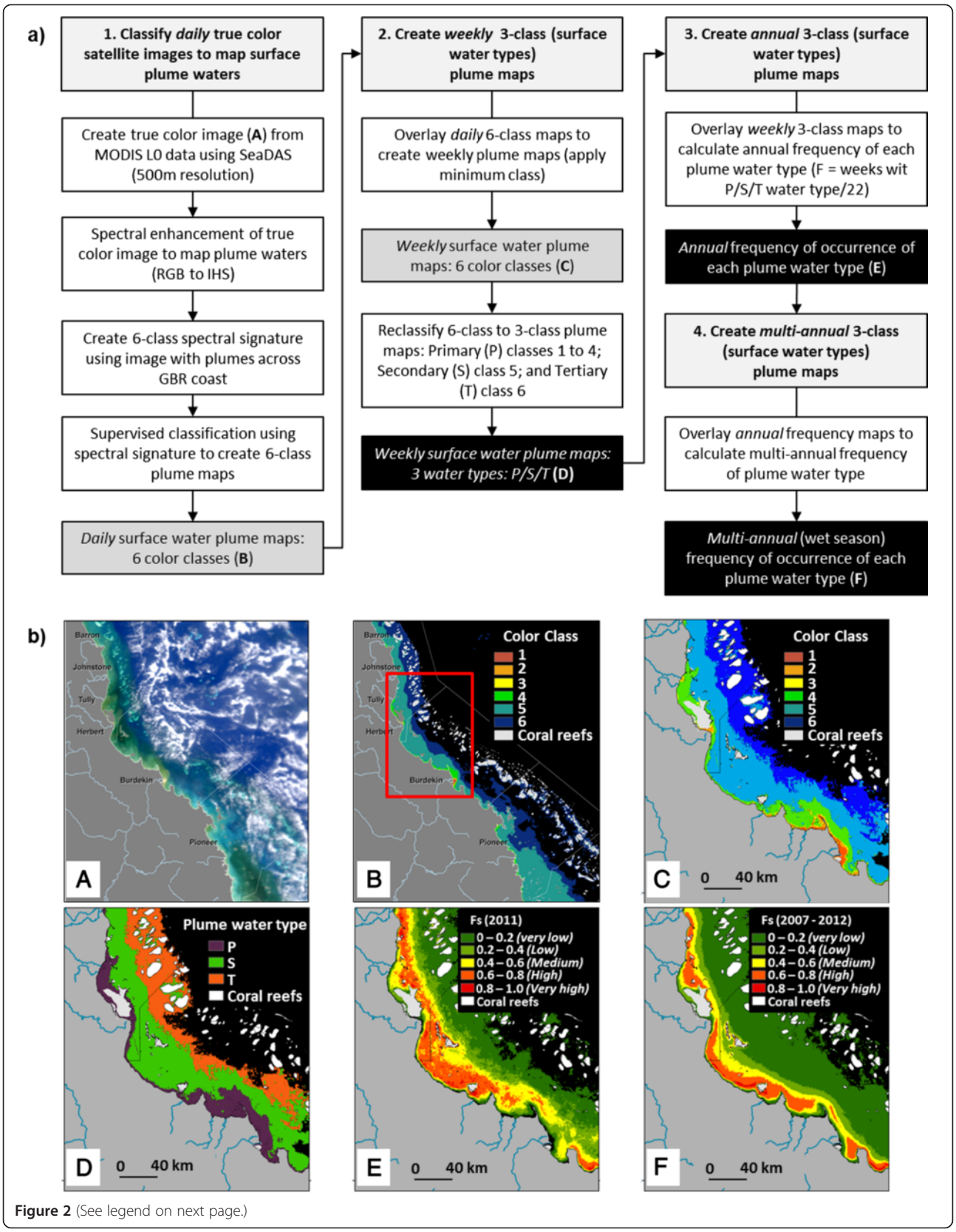

Figure 2 (See legend on next page.)

(See figure on previous page.)
Figure 2 Summary of the process followed to build plume water maps with examples of inputs and outputs. (a) Plume mapping process: different shadings represent steps (light gray), analyses within steps (white), intermediate outputs (dark gray), and final outputs (black) (modified from Álvarez-Romero et al. 2013). **(b)** A: Aqua MODIS true-colour image used to create the spectral signatures defining six colour classes for GBR plumes (25/01/2011) and B: weekly composite (19 to 25/01/2011) of six-class map (modified from Álvarez-Romero et al. 2013); C: weekly surface water plume map; D: reclassified map into weekly primary (P), secondary (S), and tertiary (T) composite (19 to 25/01/2011); E: frequency of occurrence of the secondary water type in 2011; F: multi-annual (2007–2012) frequency of occurrence of the secondary water type. Panels C–F are zoomed into the Tully-Burdekin area (see red box on panel B).

composites were assigned values of presence/absence of primary, secondary, or tertiary water type, and overlaid to generate an annual frequency map. The annual frequency of occurrence for each water type was calculated as the number of weeks that a pixel value was retrieved as primary, secondary or tertiary water type, divided by the maximum number of weeks in a wet season (i.e., 22 weeks taken from 1 December to 30 April). This overlay of water type imagery created annual (wet season) frequency maps of occurrence to primary (f_p), secondary (f_s), and tertiary (f_t) water types for the whole GBR.

Data in the annual maps were summed to calculate multi-annual (2007–2012) frequency of occurrence for each of the three plume water types. Annual frequency values depicting the extent of the secondary waters (f_s) for each year from 2007 to 2012 were mapped for the areas between Cape York and the Fitzroy River.

Comparison and validation of the flood plume water type with in-situ water quality data

Mean annual (ca. from December to April) in-situ values of chl-a, TSS, and K_dPAR were mapped against annual frequency maps of primary, secondary, and tertiary water types for each of the 6 years (2007–2012). The water quality data (chl-a, TSS, K_dPAR) was assigned to primary, secondary, or tertiary water type where that frequency of the water type was greater than 0.5, signifying the pixel was identified as a primary, secondary, or tertiary water type for at least 50% of the wet season. The mean value (x ± standard error) of chl-a, K_dPAR, and TSS was then calculated for each water type over the sampling period (Figure 3, step i).

Over the whole GBR, TSS, chl-a, and K_dPAR data were aggregated into 20 equidistant frequency classes representing the range of normalised frequency values (0–1) for each wet season for the primary, secondary, and tertiary maps. The mean values for TSS, chl-a, and K_dPAR were calculated against each of these frequency classes for primary (f_p), secondary (f_s), and tertiary (f_t) water type (see Figure 3, step ii).

Results

Influence of flow and salinity on the chl-a and WQ concentrations

In the last 5 years from 2007 to 2013, the total annual discharge for 35 rivers distributed throughout the GBR

Table 1 Plume water types as described in Devlin et al. (2012a) and Álvarez-Romero et al. (2013), detailing the water quality and optical properties which define the plume characteristics within each plume type (e.g., Clarke et al. 1970; Morel and Prieur 1977; Froidefond et al. 2002; McClain 2009)

Colour classes	Water type	Description	Colour properties
1 to 4	Primary	Sediment-dominated waters: characterised by high values of coloured dissolved organic matters (CDOM) and total suspended sediment (TSS), with TSS concentrations dropping out rapidly as the heavier particulate material flocculates and settles to the sea floor (Devlin and Brodie 2005; Brodie and Waterhouse 2009). Turbidity levels limit the light (K_dPAR) in these lower salinity waters, inhibiting production by primary producers and limiting chl-a concentrations.	Greenish-brown to beige waters: Sediment particles are highly reflective in the red to infra-red wavelengths of the light spectrum. Sediment-dominated waters have a distinctive brown/beige colour, depending upon the concentration and mineral composition of the sediments.
5	Secondary	Chlorophyll-a-dominated waters: characterised by a region where CDOM is elevated with reduced TSS concentrations due to sedimentation. In this region, the increased light in comparison to primary water type condition (but still under marine ambient conditions) and nutrient availability prompt phytoplankton growth measured by elevated chl-a concentrations.	Bluish-green waters: Due to this green pigment, chlorophyll/phytoplankton preferentially absorb the red and blue portions of the light spectrum (for photosynthesis) and reflect green light. Chl-a-dominated waters will appear as certain shades, from blue-green to green, depending upon the type and density of the phytoplankton population.
6	Tertiary	CDOM-dominated waters: Offshore region of the plume that exhibits no or low TSS that has originated from the flood plume and above ambient concentrations of chl-a and CDOM. This region can be described as being the transition between secondary water type and marine ambient conditions.	Dark yellow waters: CDOM are highly absorbing in the blue spectral domain. CDOM-dominated waters have a distinctive dark yellow colour.

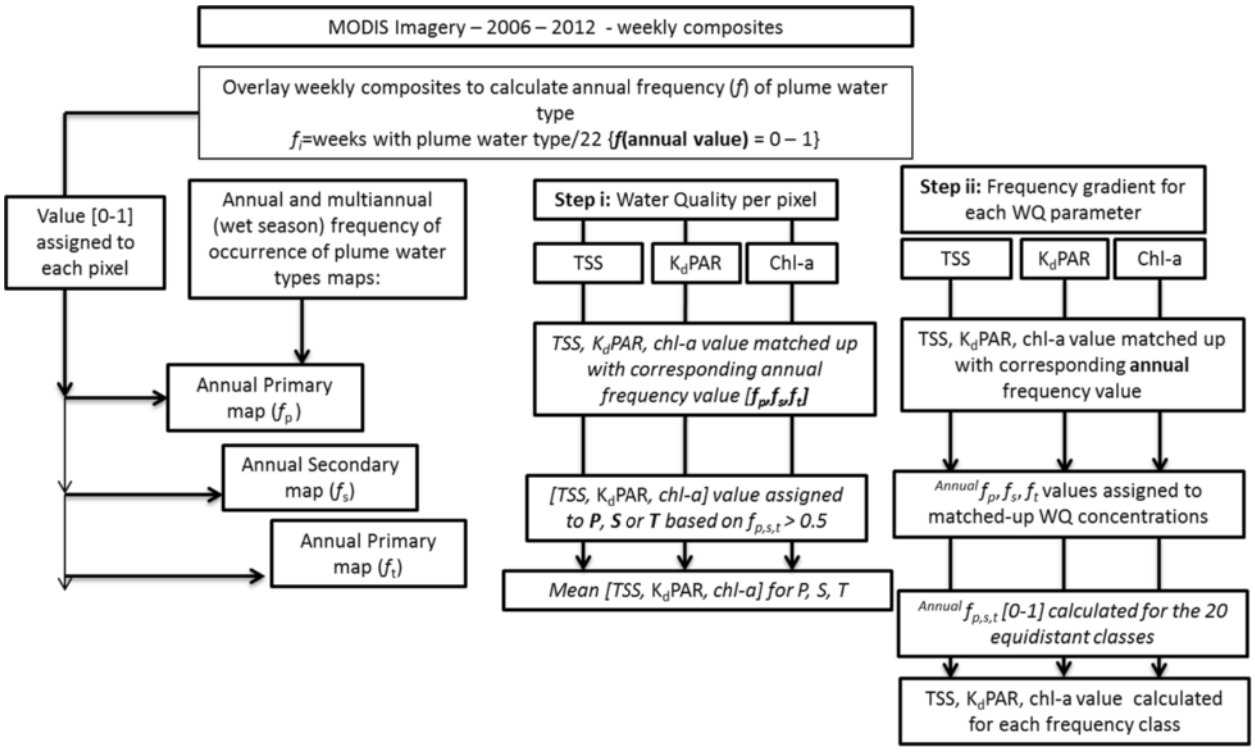

Figure 3 Summary of the process followed to compare and validate in-situ water quality concentrations with the information derived from annual and multi-annual frequency maps.

has exceeded the total annual long-term median calculated for the hydrological year (i.e., 1 October to 30 September) covering the period 1970–2000, with exceedances ranging from 66 to 620% higher than the long-term median flow (Figure 4). Record flow conditions were measured for 2010–2011, where a combination of three cyclones produced record flows in nearly all GBR rivers, particularly in the southern half of the GBR. Flows in the latter 3 years have been dominated by large floods out of the southern rivers, particularly the large dry tropic rivers, Burdekin and Fitzroy, and by the southern influence of flow from the Burnett-Mary (Devlin et al. 2012a; da Silva et al. 2013).

Sampling dates were representative of the river discharge peaks that occurred in the extended wet season (1 October to 31 May) from 2007 to 2013, considering all 35 rivers sampled over the GBR (Figure 5a) and also when Tully (Figure 5b) and Fitzroy (Figure 5c) are taken into account individually. The total maximum discharge peaks did not vary much among years, except for the 2007 and 2010 wet seasons, where flow peaks were at

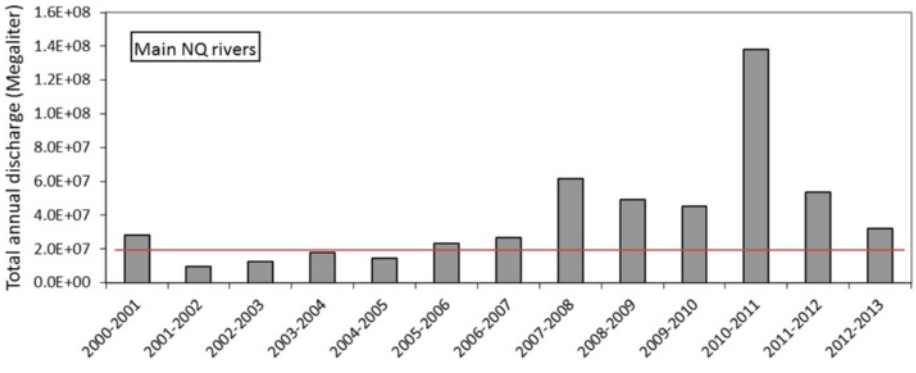

Figure 4 Total flow discharged into the Great Barrier Reef lagoon for the period from 2000 to 2013. River flow is calculated from the sum of 35 river systems which flow directly into the GBR (http://watermonitoring.derm.qld.gov.au/host.htm). Flow is measured over a water year, calculated from 1 October to 30 September. The red line denotes the long-term annual median flow (calculated from 1970 to 2000).

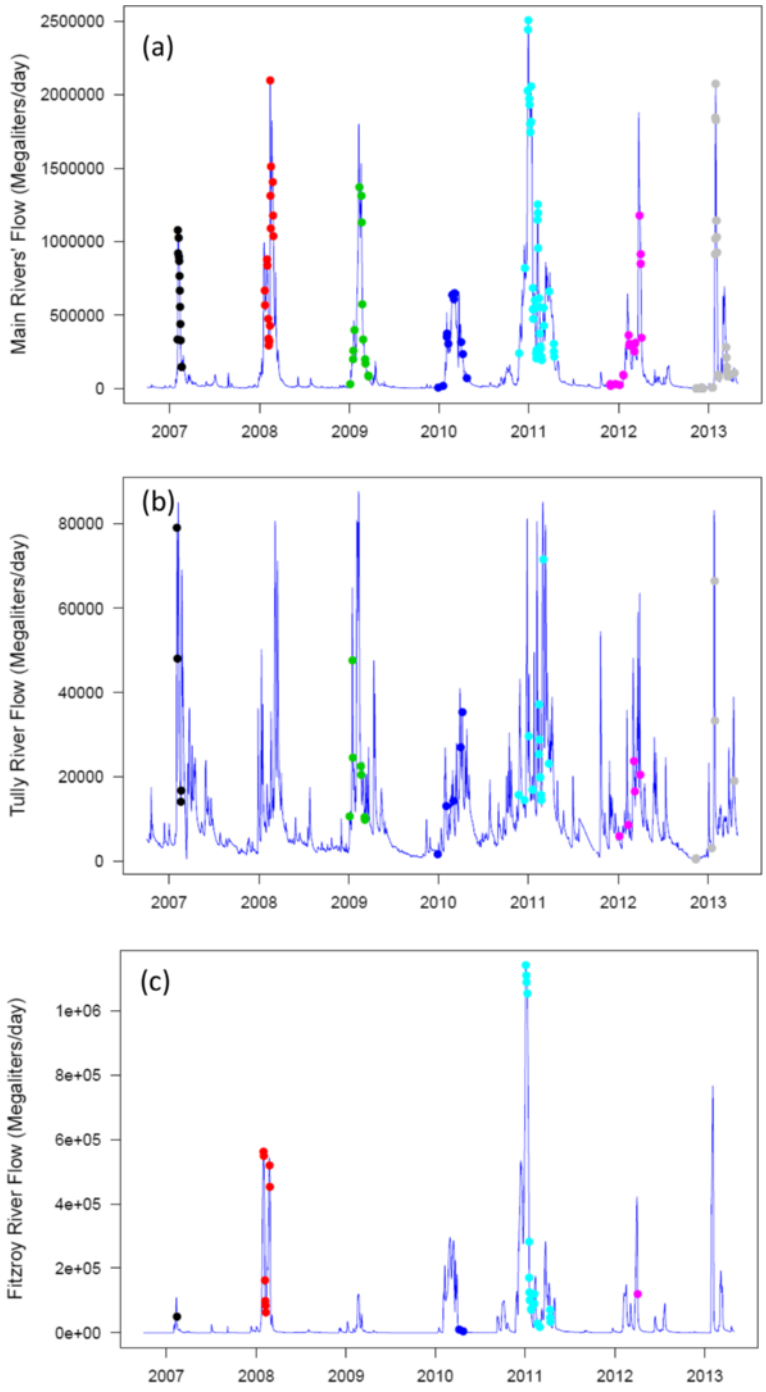

Figure 5 Flow variability for an extended wet season (ca. from 1 October to 31 May) associated with the (a) GBR, (b) Tully River, and (c) Fitzroy River. The Tully flow variability is selected as representative of a wet tropics river, with the Fitzroy River representing the dry tropics. Sampling dates over the whole GBR, Tully and Fitzroy are identified in various colours per sampling year. An extended wet season was used to guarantee coverage of any changes in the rainfall regime and to avoid plotting long periods of the year without any runoff. Note the variation in flow volume on the Y axis.

least 40% lower than in other years. Conversely, the length of the wet season varied among years, resulting in the differences in annual flow presented in Figure 4.

Concentrations of chl-a were variable across all regional transects (Table 2i), with mean chl-a concentrations ranging from 0.79 to 2.00 μg L^{-1}, reflecting the

Table 2 Statistical measures of chl-a concentration for each transect in the study

No	Region	River	Period	Min	Max	Mean	SD	*n*
i	Wet tropics	Russell-Mulgrave	2006–2013	0.21	1.60	0.79	0.49	21
		Tully	2006–2013	0.20	6.14	0.95	0.79	339
		Herbert	2006–2013	0.20	10.15	1.58	1.61	102
		Proserpine	2006–2013	0.24	3.47	0.89	0.57	46
	Dry tropics	Burdekin	2006–2013	0.20	13.78	1.07	1.54	134
		Fitzroy	2006–2013	0.20	26.70	2.00	3.49	164
ii	Wet tropics	Tully	2006–2007	0.40	3.36	1.11	0.60	26
			2007–2008					
			2008–2009	0.20	2.24	0.72	0.52	46
			2009–2010	0.20	2.70	0.79	0.50	54
			2010–2011	0.20	6.14	1.11	1.00	145
			2011–2012	0.27	3.74	0.75	0.65	47
			2012–2013	0.23	1.66	0.90	0.41	21
iii	Wet tropics	Herbert	2006–2007					
			2007–2008					
			2008–2009					
			2009–2010					
			2010–2011					
			2011–2012	0.20	10.15	1.63	1.72	85
			2012–2013	0.29	2.90	1.35	0.92	17
iv	Wet tropics	Burdekin	2006–2007	0.20	13.78	1.27	2.24	52
			2007–2008	0.20	3.47	1.08	0.78	40
			2008–2009	0.20	0.99	0.33	0.19	18
			2009–2010	0.69	3.40	1.91	1.34	5
			2010–2011	0.20	2.67	1.03	0.87	18
			2011–2012					
			2012–2013	0.75	0.75	0.75		1
v	Wet tropics	Fitzroy	2006–2007	0.31	1.19	0.64	0.38	5
			2007–2008	0.20	26.70	4.18	5.61	34
			2008–2009					
			2009–2010	0.20	1.60	0.81	0.51	12
			2010–2011	0.20	22.43	1.66	2.70	99
			2011–2012	0.20	2.14	0.59	0.50	14
			2012–2013					

(i) Data grouped over all years (2006–2013) within each transect. Sampling period is constrained for the months December to April inclusive. Transect is defined by location of closest river influence. Annual statistical measurements of chl-a concentrations are also presented for (ii) Tully, (iii) Herbert, (iv) Burdekin, and (v) Fitzroy.

highly variable productivity associated with sampling across the wet season and within nutrient-rich plumes. Mean chl-a concentrations presented for the four regions ranged from 0.33 to 4.18 μg L^{-1} (Table 2ii-v) across the sampling period for all years. A Kruskal-Wallis ANOVA test identified significant differences between chl-a concentrations across regions (chi-squared value = 20.545, df = 5, $p < 0.001$) and over the sampling years (chi-squared value = 31.841, df = 6, $p < 0.001$).

Chl-a concentrations measured at each region were compared across variable flow conditions and salinity ranges (Figure 6). With the exception of the Herbert River, a significant difference for all rivers was identified at $p < 0.02$ for comparisons of flow regime by a Kruskal-Wallis ANOVA test (Table 3). The highest median concentrations were associated with the highest flow regimes (> 95%) for the Tully (0.95 μg L^{-1}) and Fitzroy (0.5 μg L^{-1}) rivers. Variations in chl-a concentrations did not show dependence on inflow

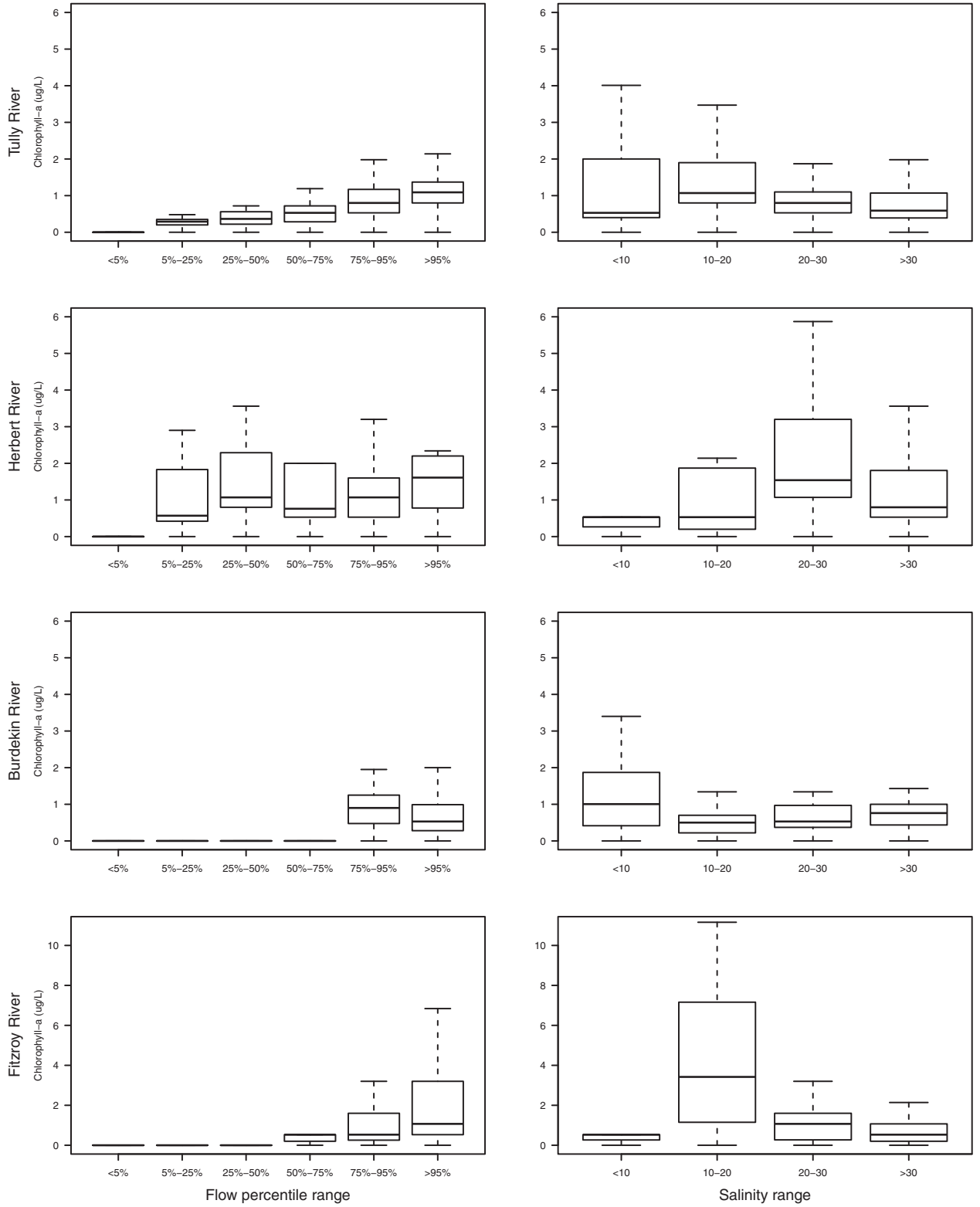

Figure 6 Chlorophyll-a concentrations across flow conditions and salinity ranges. Flow conditions are classified by percentile flow based on the long-term data from each river. Box plot presents the median (dark black line), the 25th and 75th percentiles (rectangle), and three standard deviations (vertical dashed lines).

Table 3 The ANOVA Kruskal-Wallis summary, comparing flow and salinity, over the four regions

Region	Flow			Salinity		
	Chi-squared value	*p*-value	DF	Chi-squared value	*p*-value	DF
Tully	76.6701	$p < 0.001$	4	24.3885	$p < 0.001$	3
Herbert	6.7055	$p = 0.152$	4	11.7162	$p = 0.008$	3
Burdekin	6.0687	$p = 0.014$	1	10.0161	$p = 0.018$	3
Fitzroy	10.8935	$p = 0.004$	2	24.2618	$p < 0.001$	3

regimes in the Herbert region, where no significant difference across flow regimes was detected ($p = 0.15$, Table 3). Samples taken in the Burdekin River did not cover all flow conditions, but large flows out of the Burdekin tend to flow above median conditions (> 75%) for several days during wet season sampling, making it difficult to sample along a flow continuum. Chl-a concentrations through salinity ranges were significant across the regions (Table 3), however peak median concentrations in Tully [1.4 μg L^{-1} (0.1–3.8), mean range)], Herbert [1.6 μg L^{-1} (0.1–5.9)] and Fitzroy [3.9 μg L^{-1} (0.1–10.5)] were recorded at mid salinity ranges (10–20, 20–30). The highest chl-a concentrations in Burdekin were measured in the low salinity grouping [1.0 μg L^{-1} (0.1–32)].

High frequency sampling in coastal waters under influence of the Tully River (Figure 7) allowed further elucidation of the seasonal patterns of chl-a concentration. Chl-a concentrations in Tully River plumes measured from 0.1 to 9.74 μg L^{-1} (1.91 ± 4.6 μg L^{-1}, mean ± 1 SD) over the 7 years. Repeated sampling over a range of flow conditions during the wet seasons showed the range of chl-a concentrations was higher above the threshold value of 0.45 μg L^{-1} (GBRMPA 2010) 79% of the time (i.e., 357 occurrences of 452 sampling occasions). Comparison of the mean chl-a value per sampling year with the recommended water quality guidelines (GBRMPA 2010) shows the average wet season value consistently was above this threshold (Figure 8).

Mapping the water types in flood plumes

Multi-annual plume frequency maps for a 7 year period (2007–2012) are presented for each plume type over the extent of the GBR (Figure 9). The extent of the primary water type (f_p) was variable across regions and cross-shelf, reflecting the intensity, duration, and constituent concentrations of the river discharge, but limited to a small near-shore zone (< 10 km across the shelf). On average, 5,000 km^2 of the GBR lagoon was covered by primary plume waters no less than 50% of the time.

The extent of the secondary and tertiary flood plume frequency (i.e., f_s and f_t), rarely could be attributed to an individual river, particularly from wet tropics rivers which can merge into one heterogeneous plume. Most of the time the secondary plume waters covered 25,000 km^2 of the GBR lagoon and tertiary plume waters covered 43,000 km^2.

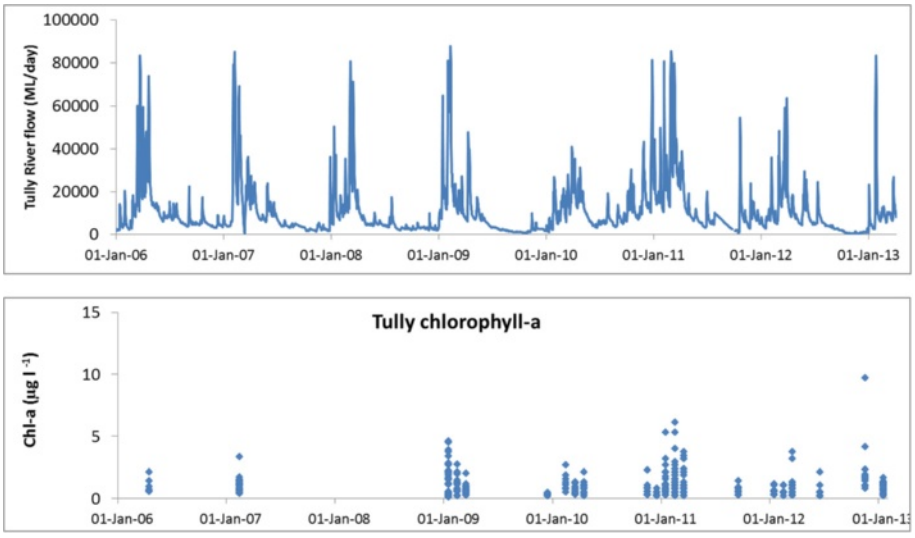

Figure 7 Flow variability for the Tully River over the sampling period with concurrent in-situ chl-a concentrations for 40 sampling occasions within the Tully marine area between the 2006/7 to 2012/3 wet seasons.

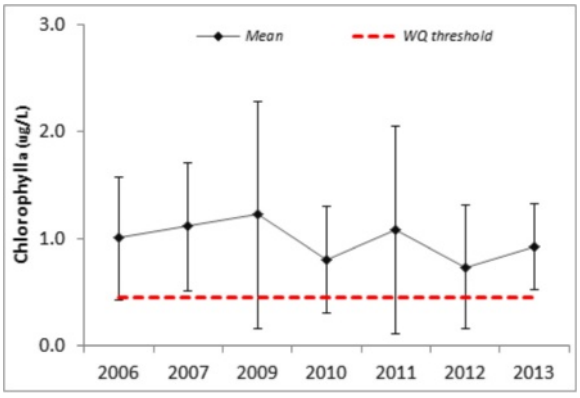

Figure 8 Annual mean chl-a concentration measured per year (excluding the 2007/8 wet season) in the Tully marine region. Dotted red line represents the annual water quality guideline for inshore waters (GBRMPA 2010). The guideline represents an annual average but is used to demonstrate the distribution of high chl-a during wet season conditions.

Comparison and validation of the flood plume water type with in-situ water quality data

In-situ water quality concentrations (chl-a, TSS, K_dPAR) were assigned to a frequency class based on the dominant water types [f_p, f_s, or $f_t > 0.5$]. The variation of concentrations in the three water quality parameters among the three water types showed a strong water quality gradient over multi-annual time-scales (e.g., as described in Devlin and Schaffelke 2009 and Devlin et al. 2012a) (Figure 10). TSS concentrations were highest in the lower salinity zone close to river mouths, and concentrations decreased through the three flood plume water types [mean ± 1SD for TSS (f_p, f_s, f_t) = 36.8 ± 5.5, 8.9 ± 3.2, 7.0 ± 4.4 mg L^{-1}]. This pattern reflected the sedimentation of the heavier particles as the water moved away from the river mouth, with only the finer colloidal sediment moving further offshore (Bainbridge et al. 2012). In contrast, the chl-a concentration was lower in the primary waters, suggesting that phytoplankton growth was reduced through light limitation (mean $K_dPAR = 0.70 \pm 0.54$) in the initial turbid primary water type (Devlin and Schaffelke 2009) and increased through the secondary water type with increasing sedimentation and nutrient availability (Figure 10). The concentrations were lower in the tertiary zone, suggesting dilution processes and biological uptake as the flood plume aged over time and space [mean ± 1SD, chl-a (f_p, f_s, f_t) = 0.98 ± 0.2, 1.3 ± 0.6, 0.7 ± 0.3 μg L^{-1}].

Figure 11 represents the mean value for each water quality parameter (TSS, K_dPAR, and chl-a concentration) plotted against increasing frequency values for the three water types. In these plots a frequency of 1 ($f_{[1.0]}$) means a location was occupied by a particular water type 100% of the time, and $f_{[0.5]}$ means a location was occupied by that type half the time. Mean concentrations of TSS in primary waters rose with increasing occurrence of primary plumes (i.e., $f_{p\ [0–0.2]} < 5$ mg L^{-1} to $f_{p\ [0.8–1.0]} > 25$ mg L^{-1}). The highest TSS concentrations related to an area where primary waters have occurred more than 80% of the time and were likely to have TSS values of greater than 25 mg L^{-1} during the wet season. TSS showed an inverse

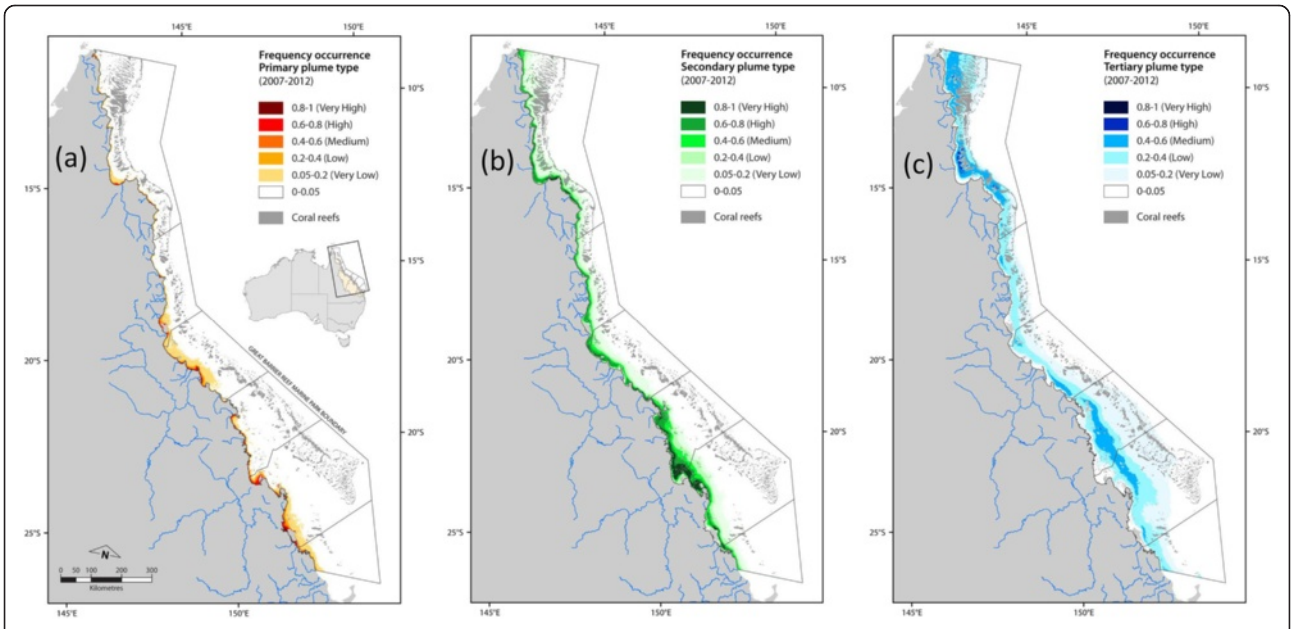

Figure 9 Multi-annual maps of primary, secondary, and tertiary plume water types in the GBR (2006–2012). Note plumes were not contemporaneous but occurred from Dec 2010 to April 2011 inclusive. The multi-annual frequency of plumes is based on a 22 week period between December and April, combined over the 6 years and were mapped for **(a)** primary, **(b)** secondary and **(c)** tertiary plume waters.

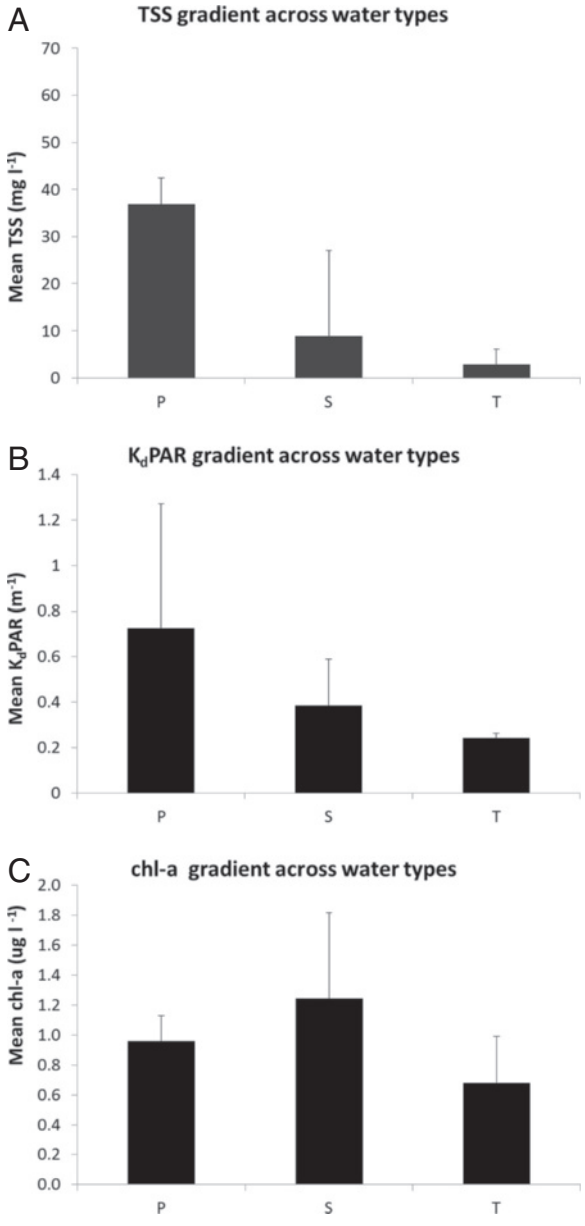

Figure 10 Mean concentrations of in-situ water quality measurements within each plume type. Water quality data were assigned to plume water type based on dominant frequency (frequency > 0.5). Data are reported for **(a)** total suspended solids (TSS), with higher values in the primary plume zone, **(b)** K_dPAR, with higher values in the primary plume zone, and **(c)** chl-a, with highest values in the secondary plume zone.

relationship in the secondary waters where mean TSS values of greater than 15 mg L^{-1} [$f_{s\ [0.0–0.2]}$] fell to less than 10 mg L^{-1} [$f_{s[0.7–1.0]}$] with reduced error around the mean at higher frequencies of occurrence of secondary plumes.

Assessment of light attenuation (K_dPAR) was partially compromised due to reduced number of in-situ measurements but followed the general trend exhibited by TSS (Pearson's correlation = 0.677, n = 298). In general, K_dPAR presented a variable pattern with values greater than 0.6 m^{-1} [$f_{P[0.65]}$] to 1.9 m^{-1} [$f_{P\ [0.9]}$] in the areas with high occurrence of primary waters. Mean values of K_dPAR ranged from 0.2 m^{-1} [$f_{s[0.1]}$] to 1.2 m^{-1} [$f_{s\ [0.05]}$] across the frequency classes of secondary waters and remained low (K_dPAR < 0.6) for the reduced number of classes measured in tertiary waters.

The mean concentrations of chl-a varied from 0.6 μg L^{-1} [$f_{P\ [0.95]}$] to 3.7 μg L^{-1} [$f_{P\ [0.45]}$] across the frequency classes of primary waters and from 0.7 μg L^{-1} [$f_{s\ [0.15]}$] to 2.7 μg L^{-1} [$f_{s\ [0.5]}$] across the secondary classes. In the tertiary waters, values dropped from 1.6 μg L^{-1} [$f_{t[0.15]}$] to less than the water quality threshold value of 0.45 μg L^{-1} [$f_{t[0.55]}$]. The variation in the chl-a concentrations in the primary and secondary waters showed a maximum peak around $f_{[0.5]}$, which was not observed for the tertiary waters. These increased chl-a concentrations for primary and secondary plume waters suggest that locations 'sharing' primary and secondary waters benefitted from the reduced light-limiting conditions characteristic of secondary waters and the availability of nutrients from the primary plume waters.

Mapping areas with high chl-a concentrations

Mapping the annual frequency of the secondary water type (Figure 12) gave a qualitative estimate of the area, where high concentrations of chl-a occurred during wet season conditions from 2006 to 2012. Secondary plumes, as mapped using this method, represent surface plume waters characterised by moderately elevated TSS with sufficient light and excess nutrients to support elevated phytoplankton growth (thus observable as green water masses).

Identifying the full extent of these secondary waters on a weekly basis provided recurrent production maps and identified the area in which high phytoplankton biomass production occurred during the variable wet season conditions (Figure 13a). The extent of the secondary flood plume on a weekly basis varied from 1,163 to 9,433 km^2. The area of the secondary flood plume was correlated with the Tully daily flow (Figure 13b). For example, the first flush of the wet season resulted in a secondary flood plume extent of 6,012 km^2, with a lag of 1 week between high flow and full extent.

Discussion

Simple indices of phytoplankton biomass, as measured by chl-a, provide an accurate means of quantifying broad-scale water quality within the Great Barrier Reef region. These data can be used as a baseline for ongoing investigation of impacts of increased nutrient discharges into Great Barrier Reef waters, such as assessing the role of altered water column nutrient status on COTS outbreaks

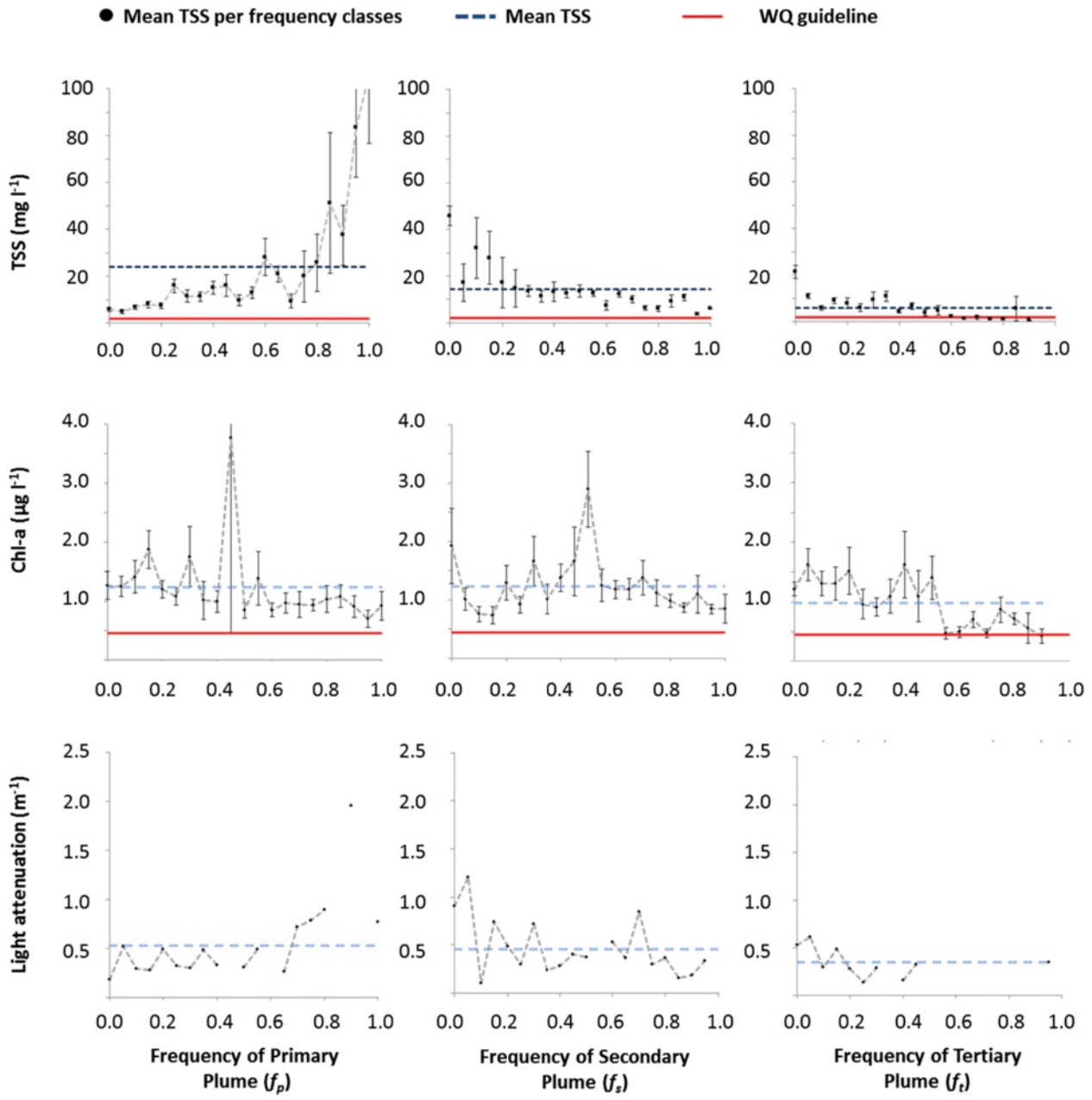

Figure 11 Plots representing mean concentrations (± SE) of TSS, chl-a, and K_dPAR, calculated for each annual frequency class for primary (f_p), secondary (f_s), and tertiary plume frequencies (f_t). Annual frequency values were calculated from the frequency of each plume type occurring over a 22 week period normalised to a value range of 0–1 and averaged over the 6 year period. The red lines for TSS and chl-a are the annual water quality guidelines for the GBR (GBRMPA 2010). The dashed line is the mean water quality value over all frequency classes.

and the influence of agriculture and urban coastal settlement on regional water quality.

The onset of the wet season and high flow conditions provides nutrient-rich waters that can nourish and enhance phytoplankton growth. The magnitude and timing of flow are important co-factors in the distribution of flood waters and the range of water quality concentrations measured over the sampling period. Inner-shelf reefs of the wet tropics region—an area of high rainfall (1,200–4,000 mm average annual)—are exposed regularly (one to several times per year) to land-based pollutants via flood plumes (Devlin et al. 2001; Devlin and Schaffelke 2009; Lewis et al. 2012), while inner-shelf reefs of the regions to the south of the wet tropics (i.e., Burdekin, Mackay, Fitzroy, and Burnett regions) are exposed less frequently but to larger flood plumes that often travel great

distances (Devlin et al. 2011, 2012a, b). Flow conditions have always been variable, however there is a strong consensus that we are now seeing the impacts from more extreme weather conditions through these higher flow conditions (Elmhirst et al. 2009; Johnson et al. 2013).

Comparative analysis of phytoplankton biomass measured in plume conditions with co-factors such as flow and salinity (Figure 6) is key information for understanding the response of phytoplankton standing stock to the input of nutrient-enhanced flood waters. Mean concentrations of chl-a measured in the flood plumes (Figure 8) (0.77–2.55 μg L^{-1}) are higher than the annual water quality guideline (0.45 μg L^{-1}, GBRMPA 2010). The highest concentrations were recorded during high peak flows (Q_{95}; Figure 6) for the Tully, Burdekin, and Fitzroy rivers. The Herbert River also showed high concentrations at lower flow quartiles (Q_{05}, Q_{10}), potentially reflecting the complex hydrodynamics around Hinchinbrook Island and the southern influence of the Burdekin River. First flush events, even at low flow conditions, are responsible for the increased delivery of dissolved inorganic nitrogen into the coastal zone (Devlin and Schaffelke 2009) from rivers with catchments containing large areas of fertilised cropland (Mitchell et al. 2009). These higher values at lower flow quartiles also suggest that the productivity in the coastal system is enhanced outside of the high flow periods. High chl-a in low river discharge conditions can be driven by sediment resuspension events in shallow waters (depth less than 10 m) where dissolved inorganic nitrogen and dissolved inorganic phosphorus mineralised from particulate nitrogen and phosphorus in benthic sediment are injected back into the water column (Chongprasith 1992; Walker 1981; Muslim and Jones 2003; Ullman and Sandstrom 1987). Resuspension of benthic sediment during cyclonic conditions occurs down to depths of 30 m and also causes phytoplankton blooms on the GBR shelf (Furnas 1989).

Over the wet season, however, the dominant driver of high chl-a concentration is the delivery of nutrient-enriched river waters. A comparison of daily flow data

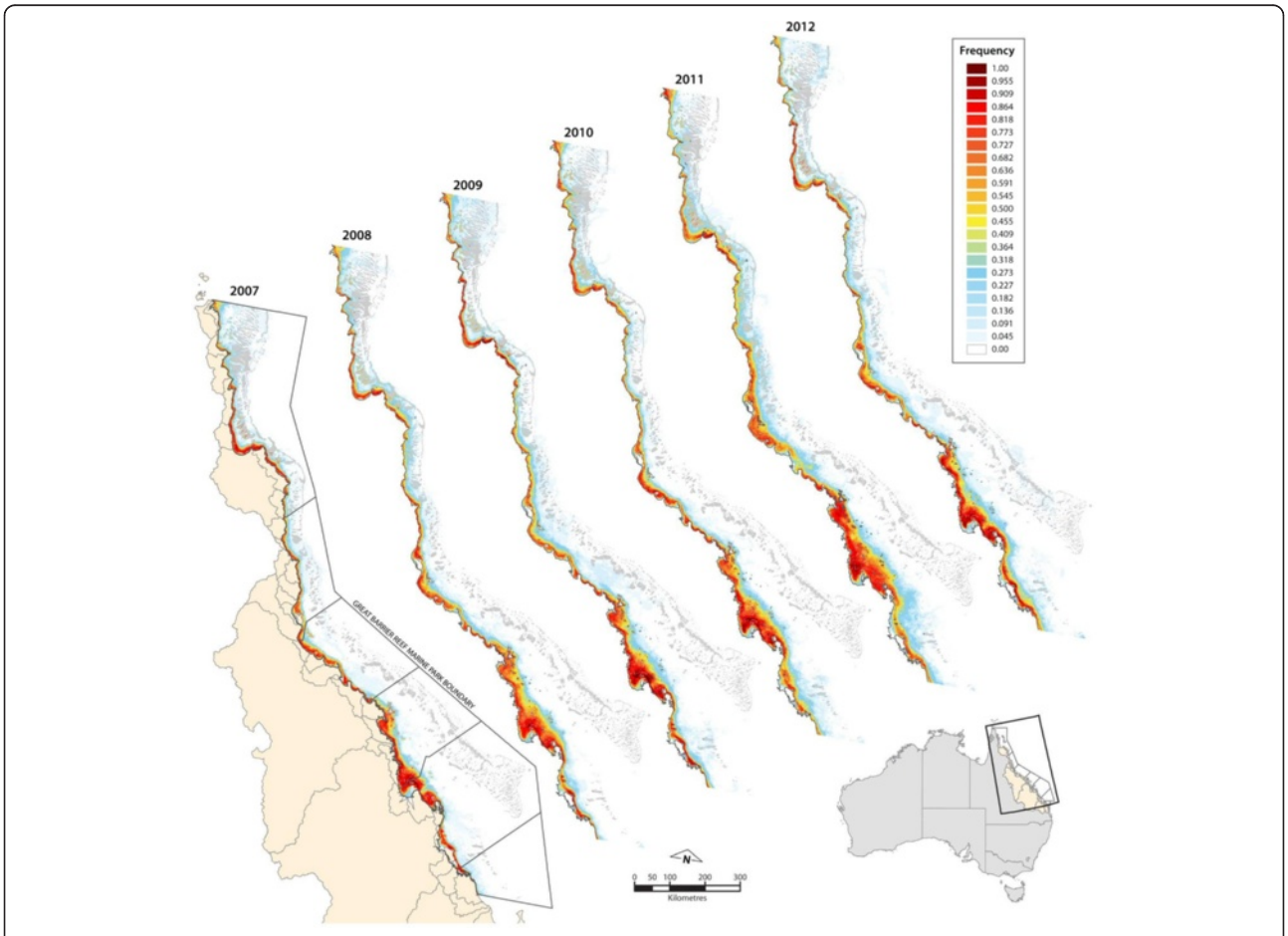

Figure 12 Areas of high chl-a biomass (identified as secondary plume waters) for each sampling year. Secondary plume water was identified from MODIS true-colour imagery (see Álvarez-Romero et al. 2013). Frequency of plumes was based on a 22 week period between December and April. Plume frequency was calculated as an averaged normalised value representing 22 weeks in each wet season.

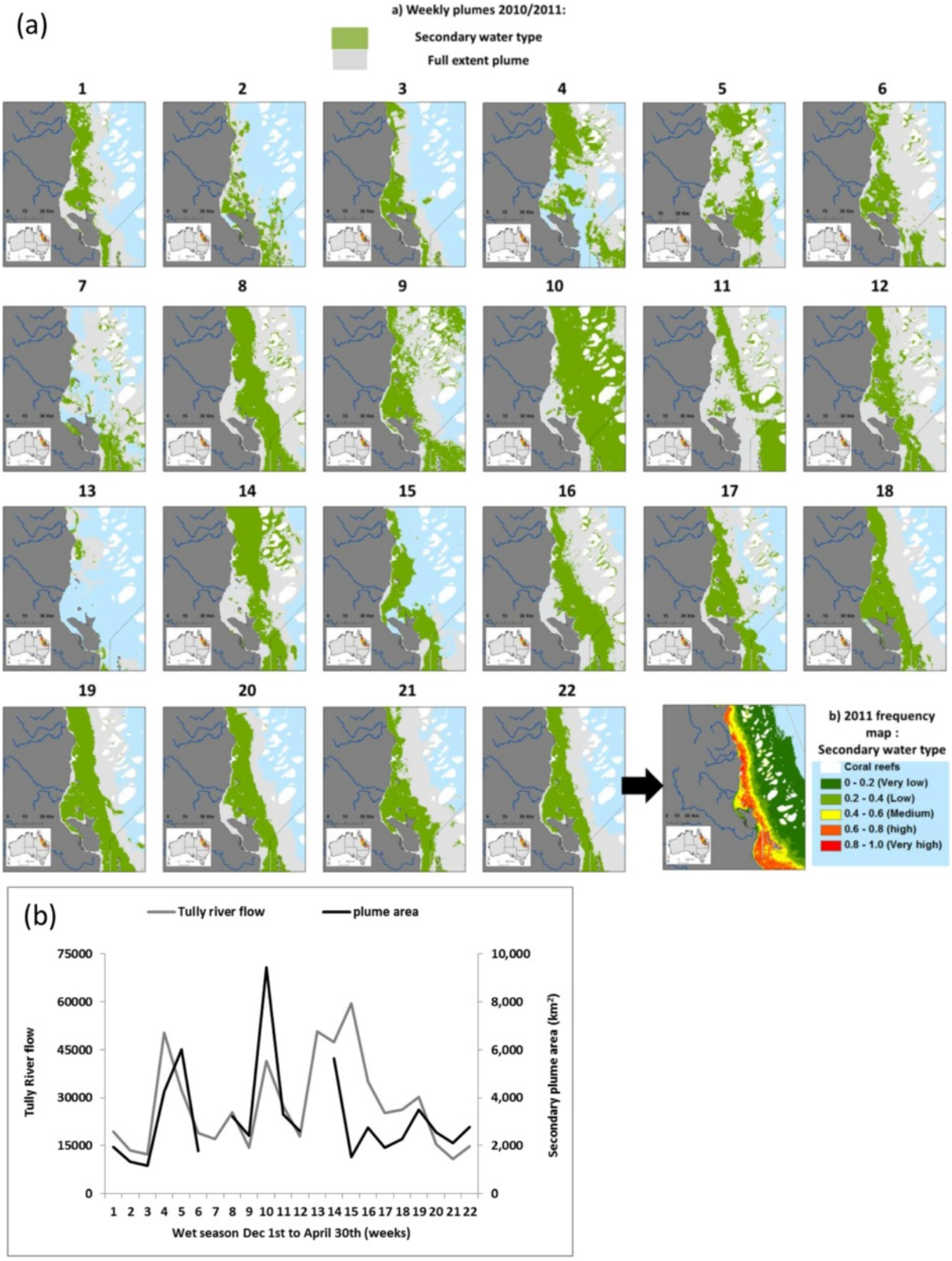

Figure 13 (See legend on next page.)

(See figure on previous page.)
Figure 13 The extent of the secondary plume in the Tully-Murray marine region over 2010/2011 wet season, including. (a) The area of secondary plume map aggregated over each week. **(b)** Area of plume (km^2) is presented for each week from week 1 (1–7 Dec 2010) to week 22 (23–30 April 2011). Daily flow data (ML/day) are shown for the same period for the Tully River (data from Department of Environment and Resource Management).

from the Tully River with daily in-situ chl-a data for the period 2006–2013 showed peaks in river flow are highly correlated temporally with elevated chl-a concentrations (Figure 7). Using data collected with high frequency for one key catchment shows that chl-a concentration is high in comparison to the GBRMPA annual guideline (GBRMPA 2010) and elevated above other reported concentrations (Brodie et al. 2007; Schaffelke et al. 2012; Figure 8). The recommended GBRMPA water quality guideline for chl-a is an annual mean measurement and, as such, is not directly comparable against chl-a data collected through the wet season only. However it does provide a reference at which to compare the chl-a data collected in the high flow periods over multiple wet seasons and illustrates the higher values measured within the wet season in the Tully marine region. Brodie et al. (2007) reported on a long-term Great Barrier Reef chl-a monitoring program which demonstrated a significant cross-shelf difference in chl-a concentrations. Data from this program also highlighted a strong regional pattern, where the inshore wet tropics had high wet season concentrations in comparison to the northern and southern transects. Brodie et al. (2007) suggested this variation in baseline and seasonal chl-a concentration was related to the differences in catchment loads where fertilised agriculture in the wet tropics contributed to high concentrations of dissolved inorganic nitrogen in riverine flow (Kroon et al. 2012; Brodie and Waterhouse 2012; Wooldridge et al. 2006). In the Tully River nitrogen concentrations rose significantly in the period 1987–2000 (Mitchell et al. 2001). Particulate nitrogen concentrations doubled and nitrate concentrations increased by 16% over this period (Mitchell et al. 2001, 2009). The cropping activities, primarily sugar cane cultivation, are concomitant with high fertiliser application rates and higher nutrient delivery in the rivers (Brodie and Mitchell 2005, Brodie et al. 2013; Kroon et al. 2012; Waterhouse et al. 2012).

The frequency of water types across the flood plume is comparable with our current understanding of water quality gradients and supports the validity of the classification method applied in this study. The higher frequency associated with the primary flood plume water type (f_p) reflects the intensity, duration, and constituent concentrations of the river discharge but is limited to a small near-shore zone (< 10 km across the shelf). These characteristics are strongly linked to the catchment hydrology and land use practices. For example, the two larger catchments over the GBR, which are under extensive agricultural development (i.e., Burdekin and Fitzroy rivers, which have greater than 80% of area utilised for agriculture), are associated with a larger area of turbid primary waters.

Secondary and tertiary plume frequency (i.e., f_s and f_t) cannot always be attributed to an individual river, particularly in the case of wet tropics rivers, which can merge into one heterogeneous plume. The area of secondary flood plume types is influenced by the onset of the primary plume through the river discharge and the local hydrodynamic conditions, mainly controlled by tides (e.g., Valente and da Silva 2009), wind regime (Dzwonkowski and Yan 2005; Lihan et al. 2008), bathymetry (e.g., Lee and Valle-Levinson 2013), and Coriolis force (Geyer et al. 2004). Mapping the annual frequency of the secondary water type (Figure 12) gave a qualitative estimate of the area where high concentrations of chl-a have occurred during wet season conditions between 2006 and 2012.

The chl-a concentration distribution is variable through the three water types, and in both primary and secondary flood plume plots, there is a peak of concentration where f_p and f_s equal 0.5, suggesting that there is a transition zone between these two water types that presents optimal environmental conditions leading to high chl-a concentrations. Figure 11 suggests that these chl-a peaks are driven by a reduction in both TSS and K_dPAR values. Waters dominated by primary (e.g., $f_p > 0.8$) or secondary (e.g., $f_s > 0.8$) plumes usually exhibit lower chl-a concentrations compared to waters where plume type is more variable (e.g., f_p or $f_s < 0.6$).

These transitional conditions potentially represent an ocean front where the denser water under-rides lighter water, giving rise to an inclined interface and a strong convergence at the surface, which can concentrate phytoplankton and pollutants (Klemas 2012).

In complex coastal areas, field data and ecological evidence are very difficult to acquire because of the temporal variability in spatial patterns of all ecological conditions and biophysical drivers causing change. Flood plume water types over multi-annual (Figure 9), annual (Figure 12), and weekly (Figure 13) time scales provide synoptic information in monitoring the water quality conditions of GBR coastal waters.

Some limitations are inherent in the true-colour classification approach used to categorise plume type in this study. One limitation described in Álvarez-Romero et al.

(2013) is the presence of other surface water masses that can be confounded with plume waters. For example, Broad Sound Channel and Shoalwater Bay, north of the Fitzroy River mouth, are areas where high turbidity occurs in the absence of plumes, mostly associated with strong tidal currents (Kleypas 1996), resulting in low confidence for accurate classification. Another limitation is the use of ocean colour data alone. Stretching of the red-green-blue images produced in SeaDAS is image-dependent and, thus, true-colour classes might be inconsistent over time. Furthermore, no atmospheric correction is applied to the true-colour images and might lead to misclassification. The impact of such misclassifications on the estimation of the primary, secondary, and tertiary water type maps should be further investigated. Despite these acknowledged limitations, the utility of the classification method is corroborated by the measurements of in-situ water quality parameters among the three water types observed over multiple years (Figure 9). The field observations reveal meaningful quantitative differences when organised along the gradients of flood plumes classified with the true-colour approach.

Connections between environmental variations and ecological systems occur across a large range of interacting spatial, temporal, and organisational scales. Collecting information at temporal or spatial scales that capture the environmental frequency and variability of patterns is essential for the decision-making process (Ostendorf 2011). Remote-sensing technologies can provide the synoptic window necessary for inventory and mapping of ocean ecosystems with information at different spatial and temporal resolutions. Using remotely sensed information in conjunction with in-situ data provides complementary approaches which allow extrapolation of the site data to a larger area and, conversely, provides validation of the remote-sensing data.

Conclusions and implications for management

Mechanisms by which phytoplankton biomass is controlled within GBR waters are through a number of co-determinants including existing nutrient pools, export and import of GBR nutrients, disturbance, grazers, and physical conditions. The higher nutrient concentrations and shallower water present in the inshore areas would typically result in high episodic pulses of phytoplankton growth. However, the difference in the productivity of the inshore GBR driven by natural processes and productivity which has increased through nutrient enrichment, resulting in the accelerated growth of phytoplankton beyond a natural threshold, can be difficult to resolve.

The current marine monitoring water quality program provides valuable information on a regional basis which can be and has been used to map acute pressure from polluted river waters (Devlin et al. 2010, 2012a). The value of intensive sampling around the formation and development of flood plumes in the coastal area is essential in our understanding of the short-term influence of river flow enhanced by sediments, nutrients, and pesticides.

The more intensive sampling associated with wet season monitoring under the current Marine Monitoring Program has now measured water quality under various flow conditions over periods of days to weeks after peak flow. Use of either in-situ data or data derived from remote sensing provides information on small to large scales, but in isolation, each data source is of limited use. Combining the data across the various scales and sensor types can enhance the information from each individual source. This paper presents only one data parameter and one type of mapping output as an example of the process of integrating variable data sources. Combining information from in-situ data with remotely sensed data can allow greater extrapolation of the point data into a spatial framework (Table 4). Concentrations are driven by the intensity of the flow, with highest concentrations measured at high flow peaks. However, when coupled with the spatial data, the highest chl-a is also linked to the transitional area affected by both primary and secondary plume waters that result in increased light, which can foster phytoplankton blooms. Note that these high biomass conditions are dependent on nutrient availability and may eventually be constrained through nutrient uptake. The process of high nutrients and clearer waters resulting in high measures of chl-a in the later stages of plume development has been explored in other work (Devlin and Brodie 2005; Devlin and Schaffelke 2009).

Knowledge of the areas and types of ecosystems that are the most likely to be impacted by changing water quality can help focus our understanding on what types of ecological impacts are occurring to those systems to help inform marine, coastal, and catchment management (Brodie et al. 2012). Details of the movement of pollutants and frequency of inundation can be key measurements in attributing water quality decline to ecosystem change. Detection and monitoring of nutrient enrichment and associated impacts in the Great Barrier Reef require a focus on the analysis of long-term in-situ data (Furnas et al. 2011; Schaffelke et al. 2012) and the inclusion of data collected over high flow events. Resolving the spatial extent of nutrient-enriched waters through the measures of high chl-a requires the analysis of remotely sensed data to fully capture the wet season variability. Combining these data sources enhances the ability to describe and distinguish anthropogenic impacts from natural wet season processes in the GBR coastal system.

Table 4 Comparison of in-situ and remote-sensing data regarding spatial and temporal conditions, costs, logistics, and confidence in data retrieval

Source data	Spatial resolution	Coverage	Temporal frequency	Costs	Data type	Logistics	Degree of confidence
In-situ chl-a data	100–5,000 m	Punctual	High (daily) to low (annually)	High	Qa	- Vessels required - Dependence of weather: high	Very high
Remote sensing – MODIS TC	1,000 m; 500 m; 250 m	Synoptic	High (daily or 2/day)	Low: Satellite images; free Computer and software	Qa	- Computer and informatic scripts to automate the production of TC data - Dependence of weather: moderate; mapping is possible under moderate cloud cover and with sun glint	Moderate to high if remotely sensed data are calibrated/ validated with in-situ information
Remote sensing – MODIS level 2 chl-a products	1,000 m	Synoptic	High (daily or 2/day)	Low: satellite images; free Computer and software	QI (Qa if combined with in-situ data)	- Computer and informatic scripts to automate the production of TC data - Dependence of weather: very high; no valid information under cloud cover or sun glint	Low to high if remotely sensed data are calibrated/validated with in-situ information
Combined in-situ and TC imagery	1,000 m; 500 m; 250 m	Synoptic	High (daily or 2/day)	High in-situ costs Satellite images: free Computer and software	Qa	- Computer and informatic scripts to automate the production of TC data - Dependence of weather: moderate; mapping is possible under moderate cloud cover and with sun glint	Moderate to high if remotely sensed data are calibrated/ validated with in-situ information

Chl-a = chlorophyll-a, Qa = quantitative, QI = qualitative, TC = true colour.

Abbreviations
Chl-a: Chlorophyll-a MODIS: Moderate resolution imaging spectroradiometer; L0: MODIS Level 0 (L0) product including raw radiance counts from all bands; Level 1B: MODIS (L1B) product including calibrated and geolocated radiances; Level 2: (L2) product including geophysical product for each pixel (after application of atmospheric correction and bio-optical algorithms); GBR: Great barrier reef; COTS: Crown of thorns (Acanthaster placi); P: Primary; S: Secondary; T: Tertiary; CDOM: Coloured dissolved organic matter; Case 1 waters: Waters in which phytoplankton (with their accompanying and covarying retinue of material of biological origin) are the principal agents responsible for variations in optical properties of the water; Case 2 waters: Waters influenced not just by phytoplankton and related particles, but also by other substances, that vary independently of phytoplankton, notably inorganic particles in suspension and yellow substances.

Competing interests
The authors declare that they have no competing interests.

Authors' contributions
MD was the lead author, drafted and completed the manuscript and carried out some of the water quality analyses and integrated remote sensed outputs with water quality data. ED, CP, JR, AW all participated in manuscript development, writing and editing. ED, CP and JR carried out the analysis around the more complex modeling of water quality data and the mapping of remote sensing information over weekly, annual and multiannual scales. DT and DZ provided expertise in spatial analysis and mapping outputs. JB provided comments on the final manuscript. All authors read and approved the final manuscript.

Acknowledgements
The authors would like to thank the Department of Sustainability, Environment, Water, Population and Communities and the Great Barrier Reef Marine Park Authority for their financial support for the ongoing work in the Reef Rescue Marine Monitoring Program. We would also like to acknowledge the contribution of valuable discussions and interactions with staff within the collaborating organisations in the MMP. In addition, the field assistance and coordination from Jason and Rebecca Rowlands at Mission Beach Charters is greatly appreciated. Thank you to the reviewers and editors for comments which have greatly improved the contents of this paper.

Author details
[1]Catchment to Reef Research Group, TropWater, James Cook University, Townsville, QLD, 4811, Australia. [2]Australian Research Council Centre of Excellence for Coral Reef Studies, James Cook University, Townsville, QLD, Australia. [3]School of Marine and Tropical Biology, James Cook University, Townsville, QLD, Australia.

Received: 4 May 2013 Accepted: 4 October 2013
Published: 30 October 2013

References
Alongi DM, McKinnon AD (2005) The cycling and fate of terrestrially-derived sediments and nutrients in the coastal zone of the Great Barrier Reef shelf. Mar Pollut Bull 51:239–252

Anthony KRN, Fabricius KE (2000) Shifting roles of heterotrophy and autotrophy in coral energetics under varying turbidity. J Exp Mar Biol Ecol 252:221–253

Álvarez-Romero JG, Devlin MJ, Teixeira da Silva E, Petus C, Ban N, Pressey RJ, Kool J, Roberts S, Cerdeira WA, Brodie J (2013) A novel approach to model exposure of coastal-marine ecosystems to riverine flood plumes based on remote sensing techniques. J Environ Manage 119:194–207

Bainbridge Z, Wolanski E, Álvarez-Romero JG, Lewis S, Brodie J (2012) Fine sediment and nutrient dynamics related to particle size and floc formation in a Burdekin River flood plume, Australia. Mar Pollut Bull 65:236–248

Baith K, Lindsay R, Fu G, McClain CR (2001) SeaDAS, a data analysis system for ocean colour satellite sensors. Eos Trans AGU 82:202

Boynton WR, Hagy JD, Murray L, Stokes C, Kemp WM (1996) A comparative analysis of eutrophication patterns in a temperate coastal lagoon. Estuar Coast Shelf Sci 19:408–421

Brando V, Schroeder T, Dekker A, Park Y (2010) Reef rescue marine monitoring program: using remote sensing for GBR wide water quality. Final report for 2009/10 activities. CSIRO, Canberra

Brando V, Dekker A, Park Y, Schroeder T (2012) Adaptive semianalytical inversion of ocean colour radiometry in optically complex waters. Appl Optics 51(15):2808–2833. doi:10.1364/AO.51.002808

Bricker SB, Ferreira JG, Simas T (2003) An integrated methodology for assessment of estuarine trophic status. Ecol Model 169:39–60

Brodie JE, Furnas M (1994) Long term monitoring programs for eutrophication and the design of a monitoring program for the Great Barrier Reef. Proc 7th Int Coral Reef Symp Guam 1:77–84

Brodie JE, Mitchell AW (2005) Nutrients in Australian tropical rivers: changes with agricultural development and implications for receiving environments. Mar Freshwater Res 56:279–302

Brodie JE, Waterhouse J (2009) Assessment of the relative risk of impacts of broad-scale agriculture on the Great Barrier Reef and priorities for investment under the Reef Protection Package. In: Stage 1 Report: April 2009. ACTFR technical report 09/17. Australian Centre for Tropical Freshwater Research, Townsville

Brodie JE, Waterhouse J (2012) A critical review of environmental management of the 'not so Great' Barrier Reef. Estuar Coast Shelf Sci 104–105:1–22

Brodie JE, Furnas MJ, Steven ADL, Trott LA, Pantus F, Wright M (1997) Monitoring chlorophyll in the Great Barrier Reef lagoon: trends and variability. In: Lessios HA, Macintyre IG (eds) Proc 8th Int Coral Reef Symp 1., pp 797–802

Brodie JE, Fabricius K, De'ath G, Okaji K (2005) Are increased nutrient inputs responsible for more outbreaks of crown of thorns starfish? An appraisal of the evidence. Mar Pollut Bull 51:266–278

Brodie JE, De'ath G, Devlin MJ, Furnas M, Wright M (2007) Spatial and temporal patterns of near-surface chlorophyll a in the Great Barrier Reef lagoon. Mar Freshw Res 58:342–353

Brodie JE, Schroeder T, Rohde K, Faithful J, Masters B, Dekker A, Maughan M (2010) Dispersal of suspended sediments and nutrients in the Great Barrier Reef lagoon during river-discharge events: conclusions from satellite remote sensing and concurrent flood-plume sampling. Marine and Freshwater Research 61(6):651–664

Brodie JE, Devlin MJ, Haynes D, Waterhouse J (2011) Assessment of the eutrophication status of the Great Barrier Reef lagoon (Australia). Biogeochemistry 106:281–302

Brodie JE, Kroon FJ, Schaffelke B, Wolanski EC, Lewis SE, Devlin MJ, Bohnet IC, Bainbridge ZT, Waterhouse J, Davis AM (2012) Terrestrial pollutant runoff to the Great Barrier Reef: an update of issues priorities and management responses. Mar Poll Bull 65:81–100

Brodie J, Waterhouse J, SchaffelkeB JJ, Kroon F, Thorburn P, Rolfe J, Lewis S, Warne M, Fabricius K, McKenzie L, Devlin M (2013) Reef Water Quality Scientific Consensus Statement 2013. Department of the Premier and Cabinet. Queensland Government, Brisbane

Chongprasith P (1992) Nutrient release and nitrogen transformations resulting from resuspension of Great Barrier Reef shelf sediments. James Cook University of North Queensland, Townsville, PhD Dissertation

Clarke GL, Ewing GC, Lorenzen CJ (1970) Spectra of backscattered light from sea obtained from aircraft as a measure of chlorophyll concentration. Science 16:1119–1121

Cloern JE (2001) Our evolving conceptual model of the coastal eutrophication problem. Marine Ecol Progress Ser 210(2001):223–253

Collier CJM, Waycott M, Mckenzie LJ (2012) Light thresholds derived from seagrass loss in the coastal zone of the Great Barrier Reef. Ecol Indic 23:211–219

da Silva ET, Devlin M, Wenger A, Petus C (2013) Burnett-Mary wet season 2012–2013: water quality data sampling, analysis and comparison against wet season 2010–2011 data. Centre for Tropical Water & Aquatic Ecosystem Research (TropWATER) Publication. James Cook University, Townsville

De'ath G, Fabricius KE, Sweatman H, Puotinen M (2012) The 27-year decline of coral cover on the Great Barrier Reef and its causes. Proc Natl Acad Sci USA 109(44):17995–17999

Dennison WC, Orth RJ, Moore KA, Stevenson JC, Carter V, Kollar S, Bergstrom PW, Batiuk RA (1993) Assessing water quality with submersed aquatic vegetation. BioScience 43(2):86–94

Devlin M, Brodie J (2005) Terrestrial discharge into the Great Barrier Reef Lagoon: nutrient behavior in coastal waters. Mar Pollut Bull 51:9–22

Devlin M, Schaffelke B (2009) Spatial extent of riverine flood plumes and exposure of marine ecosystems in the Tully coastal region Great Barrier Reef. Mar Freshwat Res 60:1109–1122

Devlin M, Waterhouse J, Taylor J, Brodie J (2001) Flood plumes in the Great Barrier Reef: spatial and temporal patterns in composition and distribution.

GBRMPA research publication no. 68. Great Barrier Reef Marine Park Authority, Townsville, Australia

Devlin M, Barry J, Painting S, Best M (2009) Extending the phytoplankton tool kit for the UK Water Framework Directive: indicators of phytoplankton community structure. Hydrobiologia 633(1):151–168

Devlin M, Harkness P, McKinna L, Waterhouse J (2010) Mapping of risk and exposure of Great Barrier Reef ecosystems to anthropogenic water quality. Report to the Great Barrier Reef Marine Park Authority August 2010, Australian Centre for Tropical Freshwater Research. ACTFR report number 10/12. James Cook University, Townsville, Australia

Devlin M, Wenger A, Waterhouse J, Alvarez-Romero JG, Abbot B, da Silva ET (2011) Reef rescue marine monitoring program: flood plume monitoring annual report 2010–11. Incorporating results from the Extreme Weather Response Program flood plume monitoring. ACTFR final report 02/12. James Cook University, Townsville, Australia

Devlin M, McKinna LW, Álvarez-Romero JG, Petus C, Abott B, Harkness P, Brodie J (2012a) Mapping the pollutants in surface riverine flood plume waters in the Great Barrier Reef Australia. Mar Pollut Bull 65:224–235

Devlin M, Schroeder T, McKinna L, Brodie J, Brando V, Dekker A (2012b) Chapter 8: monitoring and mapping of flood plumes in the Great Barrier Reef based on in situ and remote sensing observations. In: Chang N (ed) Environmental remote sensing and systems analysis. CRC Press, Boca Raton, pp 147–190

Devlin MJ, Debose J, Adjani P, Brodie J (2013) Phytoplankton in the Great Barrier Reef – potential links to crown of thorns outbreaks – a review. In: Report to the National Environmental Research Program. Reef and Rainforest Research Centre, Cairns, p 44

Dzwonkowski B, Yan X-H (2005) Tracking of a Chesapeake Bay estuarine outflow plume with satellite-based ocean colour data. Cont Shelf Res 25:1942–1958

Elmhirst T, Connolly SR, Hughes TP (2009) Connectivity regime shifts and the resilience of coral reefs. Coral Reefs 28:949–957

Fabricius KE (2005) Effects of terrestrial runoff on the ecology of corals and coral reefs: review and synthesis. Mar Pollut Bull 50:125–146

Fabricius KE (2011) Factors determining the resilience of coral reefs to eutrophication: a review and conceptual model. In: Dubinsky Z, Stambler N (eds) Coral reefs: an ecosystem in transition. Springer, New York, pp 493–506

Fabricius KE, Wolanski E (2000) Rapid smothering of coral reef organisms by muddy marine snow. Estuar Coast Shelf Sci 50:115–120

Fabricius KE, Okaji K, De'ath G (2010) Three lines of evidence to link outbreaks of the crown-of-thorns seastar Acanthaster planci to the release of larval food limitation. Coral Reefs 29:593–605

Froidefond JM, Gardelb L, Guiralb D, Parrab M, Ternon JF (2002) Spectral remote sensing reflectances of coastal waters in French Guiana under the Amazon influence. Remote Sens Environ 80:225–232

Furnas MJ (1989) Cyclonic disturbance and a phytoplankton bloom in a tropical shelf ecosystem. In: Okaichi T, Anderson DM, Nemoto T (eds) Red tides: biology environmental science and toxicology. Proceedings of the First International Symposium on Red Tides, November 10–14, 1987. Elsevier Science, New York, Takamatsu, Kagawa Prefecture, Japan, pp 273–276

Furnas MJ, Brodie JE (1996) Current status of nutrient levels & other water quality parameters in the Great Barrier Reef. In: Hunter HM, Eyles AG, Rayment GE (eds) Downstream effects of land use. Queensland Department of Natural Resources, Brisbane, Australia, pp 9–23

Furnas MJ, Mitchell A, Skuza M, Brodie JE (2005) In the other 90%: phytoplankton responses to enhanced nutrient availability in the GBR lagoon. Mar Pollut Bull 51:253–265

Furnas M, Alongi D, McKinnon AD, Trott L, Skuza M (2011) Regional-scale nitrogen and phosphorus budgets for the northern (14°S) and central (17°S) Great Barrier Reef shelf ecosystem. Cont Shelf Res 31:1967–1990

Geyer WR, Hill PS, Kineke GC (2004) The transport transformation and dispersal of sediment by buoyant coastal flows. Cont Shelf Res 24:927–949

Gitelson AA, Gurlin D, Moses WJ, Barrow T (2009) A bio-optical algorithm for the remote estimation of the chl-a concentration in Case 2 waters. Env Res Lett 4:045003

Gordon H, Morel A (1983) Remote assessment of ocean colour for interpretation of satellite visible imagery: a review. In: Lecture notes on coastal and estuarine studies, vol. 4. Springer Verlag, New York, p 114

Great Barrier Reef Marine Park Authority (2010) Water quality guidelines for the Great Barrier Reef Marine Park, revth edn. Great Barrier Reef Marine Park Authority, Townsville

Great Barrier Reef Marine Park Authority (2012) Reef rescue marine monitoring program: quality assurance/quality control methods and procedures. Great Barrier Reef Marine Park. Authority, Townsville

Harding LW, Perry ES (1997) Long-term increase of phytoplankton biomass in Chesapeake Bay 1950–1994. Mar Ecol Prog Ser 157:39–52

Johnson JE, Brando VE, Devlin MJ, Kennedy K, McKenzie L, Morris S, Schaffelke B, Thompson A, Waterhouse J, Waycott M (2011) Reef rescue marine monitoring program: 2009/2010 synthesis report. Report prepared by the Reef and Rainforest Research Centre Consortium of monitoring providers for the Great Barrier Reef Marine Park Authority. Reef and Rainforest Research Centre, Cairns

Johnson JE, Maynard J, Devlin M, Wilkinson S, Anthony K, Yorkston H, Heron S, Puotinen M, Hooidonk R (2013) Resilience of Great Barrier Reef marine ecosystems and drivers of change. Scientific consensus statement. Reef Water Quality Protection Plan Secretariat, Queensland

Kennedy K, Schroeder T, Shaw M, Haynes D, Lewis S, Bentley C, Paxman C, Carter S, Brando V, Bartkow M, Hearn L, Mueller J (2012) Long term monitoring of photosystem II herbicides—correlation with remotely sensed freshwater extent to monitor changes in the quality of water entering the Great Barrier Reef, Australia. Mar Pollut Bull 65(4–9):292–305. doi:10.1016/j.marpolbul.2011.10.029

Klemas (2012) Remote sensing of coastal plumes and ocean fronts: overview and case study. J Coast Res 28(1A):1–7

Kleypas JA (1996) Coral reef development under naturally turbid conditions: fringing reefs near Broad Sound, Australia. Coral Reefs 15:153–167

Kroon FJ, Kuhnert PM, Henderson BL, Wilkinson SN, Kinsey-Henderson A, Abbott B, Turner RD (2012) River loads of suspended solids, nitrogen, phosphorus and herbicides delivered to the Great Barrier Reef lagoon. Mar Pollut Bull 65(4):167–181

Lee J, Valle-Levinson A (2013) Bathymetric effects on estuarine plume dynamics. J Geophys Res C Oceans 118(4):1969–1981

Lewis SE, Schaffelke B, Shaw M, Bainbridge ZT, Rohde KW, Kennedy K, Brodie JE (2012) Assessing the additive risks of PSII herbicide exposure to the Great Barrier Reef. Mar Pollut Bull 65(4):280–291

Lihan T, Saitoh S-I, Iida T, Hirawake T, Iida K (2008) Satellite-measured temporal and spatial variability of the Tokachi River plume. Estuar Coast Shelf Sci 78:237–249

McClain CR (2009) A decade of satellite ocean colour observations. Ann Rev Mar Sci 1:19–42

McKenzie LJ, Unsworth RKF, Waycott M (2010) Reef Rescue Marine Monitoring Program: intertidal seagrass annual report for the sampling period 1st September 2009–31st May 2010. Fisheries Queensland, Cairns

Mitchell A, Reghenzani J, Furnas M (2001) Nitrogen levels in the Tully River—a long-term view. Water Sci Technol 43:99–105

Mitchell A, Reghenzani J, Faithful J, Furnas M, Brodie J (2009) Relationships between land use and nutrient concentrations in streams draining a 'wet-tropics' catchment in northern Australia. Mar Freshwat Res 60:1097–1108

Morel A (1988) Optical modeling of the upper ocean in relation to its biogeneous matter content (Case 1 waters). J Geophys Res 93(C9):10749–10768

Morel A, Prieur L (1977) Analysis of variations in ocean colour. Limnol Oceanogr 22:709–722

Muslim I, Jones J (2003) The seasonal variation of dissolved nutrients chlorophyll a and suspended sediments at Nelly Bay Magnetic Island. Estuar Coast Shelf Sci 57:445–455

Naik P, D'Sa JE, Gomes HR, Goés JI, Mouw CB (2013) Light absorption properties of southeastern Bering Sea waters: analysis parameterization and implications for remote sensing. Remote Sens Environ 134:120–134

Novoa S, Chust G, Froidefond J, Petus C, Franco J, Orive E, Seoane S, Borja A (2012) Water quality monitoring in Basque coastal areas using local chl-a algorithm and MERIS images. J Appl Remote Sens 6:063519. doi:10.1117/1.JRS.6.063519

Odermatt D, Gitelson A, Vittorio E, Brando VE, Schaepman M (2012) Review of constituent retrieval in optically deep and complex waters from satellite imagery. Remote Sens Environ 118:116–126

Ostendorf B (2011) Overview: spatial information and indicators for sustainable management of natural resources. Ecol Indic 11:97–102

Schaffelke B, Mellors J, Duke NC (2005) Water quality in the Great Barrier Reef region: responses of mangrove seagrass and macroalgal communities. Mar Pollut Bull 51:279–296

Schaffelke B, Carleton J, Skuza M, Zagorskis I, Furnas MJ (2012) Water quality in the inshore Great Barrier Reef lagoon: implications for long-term monitoring and management. Mar Pollut Bull 65:249–260

Schroeder T, Devlin M, Brando VE, Dekker AG, Brodie J, Clementson L, McKinna L (2012) Inter-annual variability of wet season freshwater plume extent into the Great Barrier Reef lagoon based on satellite coastal ocean colour observations. Mar Pollut Bull 65:210–223

Sorokin YI, Sorokin PY (2010) Plankton of the central Great Barrier Reef: abundance production and trophodynamic roles. J Mar Biol Assoc UK 90:1173–1187

Spencer CP (1985) The use of plant micro-nutrient and chlorophyll records as indices of eutrophication in inshore waters. Netherland J Sea Res 19:269–275

Steven ADL, Pantus F, Brooks D, Trott L (1998) Long-term chlorophyll monitoring in the Great Barrier Reef Lagoon: status report 1 1993–1995. Great Barrier Reef Marine Park. Authority, Townsville

Ullman WJ, Sandstrom MW (1987) Dissolved nutrient fluxes from the nearshore sediments of Bowling Green Bay central Great Barrier Reef Lagoon (Australia). Estuar Coast Shelf Sci 24(3):289–303

Valente AS, da Silva JCB (2009) On the observability of the fortnightly cycle of the Tagus estuary turbid plume using MODIS ocean colour images. J Mar Syst 75:131–137

Walker TA (1981) Dependance of phytoplankton chlorophyll on bottom resuspension in Cleveland Bay northern Queensland. Mar Freshw Res 32(6):981–986

Wang M, Shi W (2007) The NIR-SWIR combined atmospheric correction approach for MODIS ocean colour data processing. Opt Express 15(24):15722–15733

Waterhouse J, Brodie J, Lewis S, Mitchell A (2012) Quantifying the sources of pollutants to the Great Barrier Reef. Mar Pollut Bull 65:394–406

Wooldridge S, Brodie JE, Furnas M (2006) Exposure of inner-shelf reefs to nutrient enriched runoff entering the Great Barrier Reef Lagoon: post-European changes and the design of water quality targets. Mar Pollut Bull 52(11):1467–1479

Yunev OA, Vedernikov VI, Gasturk O, Yilmaz A, Kideys AH, Moncheva S, Konovalov SK (2002) Long-term variations of surface chlorophyll a and primary production in the open Black Sea. Mar Ecol Prog Ser 230:11–28

doi:10.1186/2192-1709-2-31
Cite this article as: Devlin *et al.*: **Combining in-situ water quality and remotely sensed data across spatial and temporal scales to measure variability in wet season chlorophyll-a: Great Barrier Reef lagoon (Queensland, Australia).** *Ecological Processes* 2013 **2**:31.